Accepted Manuscript

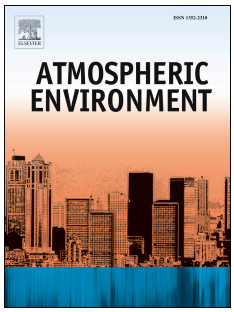

Ambient exposure to coarse and fine particle emissions from building demolition

Farhad Azarmi, Prashant Kumar

PII: S1352-2310(16)30312-0

DOI: 10.1016/j.atmosenv.2016.04.029

Reference: AEA 14572

To appear in: *Atmospheric Environment*

Received Date: 24 January 2016

Revised Date: 19 April 2016

Accepted Date: 21 April 2016

Please cite this article as: Azarmi, F., Kumar, P., Ambient exposure to coarse and fine particle emissions from building demolition, *Atmospheric Environment* (2016), doi: 10.1016/j.atmosenv.2016.04.029.

Graphical abstract

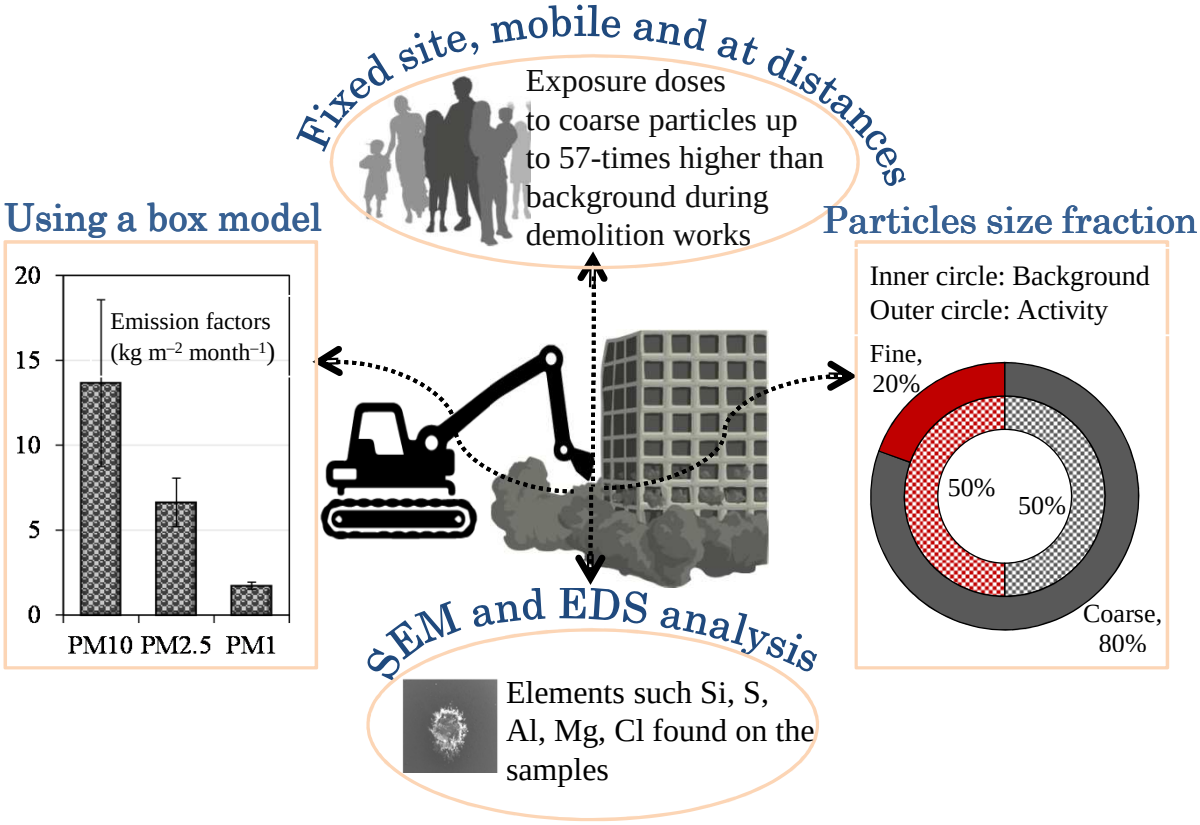

Ambient exposure to coarse and fine particle emissions from building demolition

Farhad Azarmi[a] and Prashant Kumar[a, b,*]

[a]*Department of Civil and Environmental Engineering, Faculty of Engineering and Physical Sciences, University of Surrey, Guildford GU2 7XH, United Kingdom*

[b]*Environmental Flow (EnFlo) Research Centre, Faculty of Engineering and Physical Sciences, University of Surrey, Guildford GU2 7XH, United Kingdom*

ABSTRACT

Demolition of buildings produce large quantities of particulate matter (PM) that could be inhaled by on-site workers and people living in the neighbourhood, but studies assessing ambient exposure at the real-world demolition sites are limited. We measured concentrations of PM_{10} (≤10 µm), $PM_{2.5}$ (≤2.5 µm) and PM_1 (≤1 µm) along with local meteorology for 54 working hours over the demolition period. The measurements were carried out at (i) a fixed-site in the downwind of demolished building, (ii) around the site during demolition operation through mobile monitoring, (iii) different distances away from the demolition site through sequential

[*]Corresponding author: *Department of Civil and Environmental Engineering, Faculty of Engineering and Physical Sciences, University of Surrey, Guildford GU2 7XH, United Kingdom; Tel.: +44 1483 682762; Fax: +44 1483 682135; E-mail addresses: P.Kumar@surrey.ac.uk, Prashant.Kumar@cantab.net*

monitoring, and (iv) inside an excavator vehicle cabin and on-site temporary office for engineers. Position of the PM instrument was continuously recorded using a Global Positioning System on a second basis during mobile measurements. Fraction of coarse particles ($PM_{2.5–10}$) contributed 89 (with mean particle mass concentration, PMC ≈ 133±17 μg m^{-3}), 83 (100±29 μg m^{-3}), and 70% (59±12 μg m^{-3}) of total PMC during the fixed-site, mobile monitoring and sequential measurements, respectively, compared with only 50% (mean 12±6 μg m^{-3}) during the background measurements. The corresponding values for fine particles ($PM_{2.5}$) were 11, 17 and 30% compared with 50% during background, showing a much greater release of coarse particles during demolition. The openair package in R and map source software (ArcGIS) was used to assess spatial variation of PMCs in downwind and upwind of the demolition site. A modified box model was developed to determine the emission factors, which were 210, 73 and 24 μg m^{-2} s^{-1} for PM_{10}, $PM_{2.5}$ and PM_1, respectively. The average respiratory deposited doses to coarse (and fine) particles inside the excavator cabin and on-site temporary office increased by 57- (and 5-) and 13- (and 2-) times compared with the local background level, respectively. The monitoring stations in downwind direction illustrated a logarithmic decrease of PM with distance. Energy-dispersive X-ray spectroscopy and scanning electron microscopy were used to assess physicochemical features of particles. The minerals such as silica were found as a marker of demolition dust and elements such as sulphur coming from construction machinery emissions. Findings of this study highlight a need to limit occupational exposure of individuals to coarse and fine particles by enforcing effective engineering controls.

Key words: *Occupational Exposure; Emission factors; Particulate Matter; Building demolition; SEM /EDS; Construction and demolition waste*

1. INTRODUCTION

Exposure to particulate matter (PM), including PM_{10} (≤10 μm), $PM_{2.5}$ (≤2.5 μm) and PM_1 (≤1 μm), is known to have adverse impacts on the human health (Heal et al., 2012). A number of epidemiological studies have shown excess mortality due to PM exposure from sources such as road traffic and industries (Janssen et al., 2013; Kan et al., 2007; Namdeo and Bell, 2005). Furthermore, excessive inhalation of PM_{10} and $PM_{2.5}$ has been linked to a variety of respiratory diseases, such as lung cancer (Turner et al., 2011; Vineis et al., 2004), asthmatic (Dorevitch et al., 2006; Eggleston et al., 1999), renal (Spencer-Hwang et al., 2011; Weng et al., 2015) and cardiovascular diseases (Brook et al., 2010; Peng et al., 2008), besides depression problems among construction workers (Haynes and Savage, 2007). Numerous studies have reported increased risk of death due to ischemic heart disease among construction plasterers, masons and welders (Cavallari et al., 2007; Sjogren et al., 2002; Stern et al., 2001). Similar adverse health effects have also been observed among *non-smoking* workers at construction sites (Bergdahl et al., 2004; Verma et al., 2003).

There is a reasonable amount of literature on emissions of coarse (hereafter referred to $PM_{2\text{-}5\text{–}10}$ fraction), fine ($PM_{2.5}$) and ultrafine ($PM_{0.1}$) particles from sources such as industrial works (Diapouli et al., 2013; Jaecker-Voirol and Pelt, 2000; Rodriguez et al., 2004; Toledo et al., 2008), road works (Fuller and Green, 2004; Ho et al., 2003; Tian et al., 2007; Woskie et al., 2002), road vehicles (Goel and Kumar, 2015; Kean et al., 2000; Kumar et al., 2011a, 2014) and non-vehicular activities (Kumar et al., 2013b, 2014; Saliba et al., 2010). However, there are limited studies that have measured emissions and exposure to PM around operational building demolition sites, which is the focus of this article.

Construction and demolition waste contribute up to about 33% of the total waste from all the streams; about half of which is demolition waste (Balaras et al., 2007). Construction and demolition of structures generate in excess of 450 million tonnes of waste each year in Europe, with about 53 million tonnes per year in the UK alone (Lawson et al., 2001; Rao et al., 2007). However, the number of buildings demolished each year is expected to increase by 4-fold by 2016 in the UK from the levels of about 20,000 per year in 2008 (ECI, 2005; Roberts, 2008). This increased rate of building demolition could be linked to growing population of the urban areas and the need for improvements to meet new urban design guidelines and adopt building technologies (Balaras et al., 2007; Kumar et al., 2015). For example, the global urban population is expected to increase by about 60% in 2035 from the 2013 levels (GroBmann et al., 2013; Kumar et al., 2013a).

Building demolition can be accomplished through either implosion or mechanical means (e.g. excavator and wrecking ball). Demolition by both mechanical disruption (Dorevitch et al., 2006) and implosion (Beck et al., 2003) produce significant amount of PM, but the impact of implosion demolition on surrounding areas air quality is generally short-lived and severe (Beck et al., 2003).

Recent studies have shown that workers in construction industry dealing directly with concrete and cement products are exposed to notable PM emissions (Azarmi et al., 2014; Croteau et al., 2002; Flanagan et al., 2006; Kumar et al., 2012b) compared with those working in metal and wood industries (Fischer et al., 2005; Lim et al., 2010). There are sufficient evidences that activities such as demolition, earthmoving and building renovation are important sources of PM and degrade the surrounding air quality (Azarmi et al., 2015a; Beck et al., 2003; Font et al.,

2014; Hansen et al., 2008; Joseph et al., 2009; Muleski et al., 2005). In addition, PM pollution from demolition activity can adversely impact the health of people living close to demolition sites, especially when the measures to restrict particles released from sites are inadequate (Kumar et al., 2012a). Therefore, assessment of PM exposure becomes even more important when such sites are situated within the densely built residential areas or sensitive areas such as schools and hospitals.

Understanding the chemical constituents, morphology (i.e. size, shape) and surface properties of particles released from building demolition are important for determining their toxicity and health effects (Lo et al., 2000; Senlin et al., 2008). There are techniques such as scanning electron microscopy (SEM) for analysing morphology and energy dispersive X-ray spectroscopy technique (EDS) to find elemental composition, which are used by numerous environmental studies (Kupiainen et al., 2003; Mouzourides et al., 2015; Paoletti et al., 2002). For example, Mouzourides et al. (2015) assessed the characteristics of bulk PM samples collected on Polytetrafluoroethylene (PTFE) filters at an urban air pollution monitoring station in Nicosia (Cyprus) using SEM and EDS techniques. The results showed presence of elements such as calcium (Ca), nitrogen (N) and lead (Pb) on the samples. Likewise, Paoletti et al. (2002) studied the physicochemical characteristics and composition and of particles in an urban area of Rome (Italy). They observed elements such as carbon (C) and N, mainly originated from vehicular sources. Currently, limited studies have reported physicochemical properties of particles released from the building demolition and therefore this is taken up for investigation in this study.

Health concerns related to dust inhalation have led to a number of dust control and reduction initiatives in demolition industry. The United States Environmental Protection Agency (US EPA)

104 have provided specific emission factors for different operations such as demolition, construction
105 and mineral operations to control PM emissions (EPA, 2011). In addition, the UK Health and
106 Safety Executive (HSE) developed a good practice guideline to limit exposure to hazardous
107 substances at the demolition sites (HSE, 2006, 2011). Furthermore, at local level, "Best Practice
108 Guidance" is produced by London Councils in partnership with the Greater London Authority in
109 the UK, which contains a number of practical methods to control dust and emissions from
110 demolition activities (Authority and Councils, 2006). However, demolition sites can be situated
111 within extremely busy places where meeting regulatory expectations, or strictly following
112 associated guidelines, are often challenging.

113 In order to fill the existing research gaps in the literature, this study investigates the release of
114 PM_{10}, $PM_{2.5}$ and PM_1 and associated exposure around a real-world building demolition site. The
115 aims were to: (i) quantify the emission and exposure rates of particles and their dispersion in the
116 downwind of demolished building, (ii) assess the horizontal decay of the PM emissions, (iii)
117 understand the physical and chemical properties, (iv) computation of particle mass emission
118 factors (PMEFs), and (v) determining the occupational exposure to on-site workers and people in
119 the close vicinity of the demolition site.

120 ## 2. MATERIALS AND METHODS

121 ### 2.1 Sampling set up and site description

122 PMCs were measured at the fixed-sites in the downwind of demolition site, around the
123 demolished building through the mobile monitoring as well as at different distances (10, 20, 40
124 and 80 m) from the demolition site through sequential measurements. Monitoring was also
125 carried out inside the cabin of an excavator vehicle and in on-site temporary office for engineers.

Figure 1 shows the sampling locations around the demolition site, which was situated ~10 m away from a busy road that was closed during the demolition activity (i.e. sampling period). The demolished building was 30×15×8 m (length × breadth × height) and was located in Haywards Heath in West Sussex, United Kingdom (Figure 1). Construction material of building floors, stairs and supporting columns was reinforced concrete while the walls were made of brick.

The data were collected for a total of 54 working hours between 08:00 and 18:00 h (local time) over a period of 7 days; of which, one day was without any activity that enabled us to evaluate the local background levels. Table 1 presents the detailed summary of sampling durations. The background measurements were made at 15 m from the demolition site. Fixed site measurements were made at a distance of ~10 m in the downwind of the demolition site (Figure 1) while mobile measurements were made in loops of ~100 m (route A) and ~ 600 m (route B) around the demolition site (Figure 1). We intentionally changed our mobile routes to capture the exposure of on-site workers around the demolition site (route A) and the people in nearby vicinity of the site (route B). A total of 24 runs were made at routes A and B during the demolition works; the runs were spread equally between morning and afternoon hours (Table 1).

2.2 Instrumentation

A GRIMM particle spectrometer (model 1.107 E) was used to measure the mass distribution of particles per unit volume of air in 15 different channels covering the 0.3–20 µm in size range (Goyal and Kumar, 2013). The sensitivity of the instrument is 1 µg m^{-3}, and instrument reproducibility of size-resolved PMC is ±2% over the total measuring range. Optical signals pass through a multichannel size classifier to a pulse height analyser that classifies the signals based on size into appropriate channels. Ambient air was drawn into the unit every 6

148 second via an internal volume-controlled pump at a rate of 1.2 lit min^{-1} (Goyal and Kumar,
149 2013; Grimm and Eatough, 2009).

150 Two cross validation approaches were used to ensure the quality of the collected data. Firstly, the
151 instrument was calibrated in a three-step process by the manufacturer prior to the on-site
152 measurements, including verification of laser optics, gravimetric correlation verification and
153 optical calibration against the known size-resolved distribution, density and refractive index of
154 known reference particles. This calibration used the National Institute of Standards and
155 Technology (NIST) certified polystyrene latex sphere (PSL) particles, which is a worldwide
156 accepted standard method, giving a difference between standard instrument and our unit as ~5%
157 (Supplementary Information, SI, Table S1). Secondly, we carried out on-site calibration by
158 weighing (µg) the PTFE filters that collected particle mass during the on-site measurements and
159 compared these mass with the data of PM mass produced by the instrument (see Table 2). The
160 data of the PM mass (in µg) from the instrument was obtained by multiplying the total mass
161 concentration (µg m^{-3}) with the sampling flow rate (2×10^{-5} m^3 s^{-1}) of the instrument and the total
162 duration (s) of measured activity (SI Section S1). Results of this comparison are presented in SI
163 Table S1, which shows an average difference of about 6% between the filter-based mass and the
164 mass given by the instrument. Both these approaches provided a difference of ≤6% between the
165 standard and our instruments unit, which was assumed to acceptable and no correction factor was
166 applied to the data.

167 A weather station (KESTREL 4500) was used to measure meteorological data (i.e. relative
168 humidity, barometric pressure and ambient temperature) at the sampling sites at every 10 s
169 during all the experimental campaigns. Since wind speed and direction at the sampling locations

will not be representative of the synoptic wind conditions due to being within the turbulent urban canopy layer (Kumar et al., 2011b), wind speed and direction data was acquired from the UK Met Office's weather station that was situated ~20 km away from the demolition site. The ambient average wind speed during the sampling period varied in the 0–6 m s^{-1} range, with an average wind speed of 3.0±1.5 m s^{-1} (Figure 2). The ambient temperature and relative humidity varied in the 22±2 ºC and 51±6 % range, respectively (SI Table S2). Since the variation in average temperature and relative humidity was modest, their effects on measured concentration were overlooked during the analysis.

A Global Positioning System (GPS) device (model: Garmin Oregon 350) was used to record sampling locations during the mobile measurements on a second basis (1 Hz). The data collected from the GPS in .gpx format was converted to Microsoft Excel through the map source software. Arcmap version 10.1 was used to plot spatial variations of PM_{10}, $PM_{2.5}$ and PM_1 during the different runs (Goel and Kumar, 2015).

2.3 Collection of PM mass on PTFE filters for SEM and EDS analysis

Five different samples (1-5) were collected on PTFE filters that had a diameter of 47 mm and a nominal thickness of ~1000 µg cm^{-2} (Table 2). Filter sample 1 was treated as a "blank" while mass on sample 2 was collected during the background period (pre-demolition; day 1). Mass on filter samples 3, 4 and 5 were collected during fixed-site (days 2 and 3), mobile (days 4 and 5) and sequential measurements (days 6 and 7), respectively (Section 2.1). Further details on the sampling duration and mass collected on the sampled filters are provided in Table 2.

Each of these five filter samples were analysed using a JEOL SEM (model: JSM-7100F) with a spatial resolution of 1.2 nm at 30 kV, equipped with energy dispersive X-ray spectrometer

(EDS), to obtain information on the surface morphology and composition of the particles collected on filters. The analyses were performed at The Microstructural Studies Unit of the University of Surrey (UK). The sample surface was scanned with a high-energy (~3.0 kV) beam of electrons in a raster pattern. The scanned area was between 6×6 and 200×200 μm^2 in accordance with the magnification applied (JEOL, 2015).

2.4 Estimation of PMEFs

The PMEFs are defined as the mass of emitted particles per unit area of demolition per second ($\mu g\ m^{-2}\ s^{-1}$). These were estimated for PM_{10}, $PM_{2.5}$ and PM_1 fractions separately using the data collected during the fixed-site measurements in the downwind of the demolished building (Section 2.1). A box model was initially developed, and then modified to take into account the horizontal decay of PM fractions, using the mass balance concept for the assessment of demolition-related PMEFs (Figure 3). Similar modelling approach to estimate the PMEFs has been used by previous studies (Font et al., 2014; Jamriska and Morawska, 2001; Kumar et al., 2011a).

It has been assumed that the box has a width, length and the maximum height where the pollutants mix as L, W and H_m, respectively. Formulation of the box model assumes that the demolition site acts as a control volume (box), and that the air in the box is well mixed with uniform (U_x in $m\ s^{-1}$) and exchange (U_z in $m\ s^{-1}$) wind velocities in the x– and z–directions, respectively. The model also assumes that there is no change in PMCs through transformation processes in the box (Kumar et al., 2011a). The removal of PM due to deposition and gravitational settling are assumed to be negligible.

On a dimensional basis, it is assumed that the mass flow rate ($\mu g\ s^{-1}$) due to the emissions from

the demolition site is equal to the product of PMEFs (μg m^{-2} s^{-1}) and the surface area (m^2) (Font et al., 2014).

$$\text{Mass flow rate} = \text{PMEF} \times \text{L} \times \text{W} \quad (1)$$

Further, consideration of the conservation of mass for PM gives their mass flow rate in the box as: Net mass flow rate due to demolition activity = mass flow entering and leaving the box through horizontal advection (f_x) + mass flow through vertical exchange (f_z). Eq. (1) can then be written as:

$$\text{PMEF} \times \text{L} \times \text{W} = \left[(\text{PM}_{\text{activity}} \times U_x \times H_m \times L) - (\text{PM}_{\text{background}} \times U_x \times H_m \times L)\right] + \left[(\text{PM}_{\text{activity}} \times U_z \times W \times L) - (\text{PM}_{\text{background}} \times U_z \times W \times L)\right] \quad (2)$$

Vertical exchange wind velocity is assumed to be negligible, and thus the calculation for mass flow entering and leaving the box through vertical advection was overlooked from the calculations of the particle emissions rates. With this assumption, Eq. (2) becomes:

$$\text{PMEF}_i \times \text{L} \times \text{W} = \left[(\text{PM}_{i,\text{activity}} \times U_x \times H_m \times L) - (\text{PM}_{i,\text{background}} \times U_x \times H_m \times L)\right] \quad \textit{or}$$

$$\text{PMEF}_i \times \text{W} = \Delta\text{PM}_i \left[U_x \times H_m\right] \quad (3)$$

where ΔPM_i (μg m^{-3}) is the subtraction of the PMC during the "background" period from the total PMCs measured during the "activity" period (i.e. ΔPM_i = PM (activity, downwind) – PM (background); subscript *i* of PM and PMEF refers to size fractions of PM (i.e. PM_{10}, $PM_{2.5}$ and PM_1).

Since the measurements were taken at ~10 m away from the site, there will be a *dilution* between the source (i.e. demolition site) and the monitoring station. Hence the emission factors using these measured concentrations at a distance away from the source will underestimate the PMEFs.

Therefore, the horizontal decay profiles (Eq. 4) were developed through our sequential measurements in Section 3.4 to account for the dilution between the emission source and sampling location, and back-calculate PM_{10}, $PM_{2.5}$ and PM_1 concentrations closest (~0.1 m away from demolition site) to the emission source before putting them in Eq. (3).

$$\Delta PM_i = -a \ln(x) + c \quad (4)$$

where x (m) is a distance from the demolition site. The values of the empirical coefficient a (µg m^{-4}) are 13.57, 8.51 and 1.77 for PM_{10}, $PM_{2.5}$ and PM_1, respectively (Section 3.4). Likewise, c (–) is a constant with values as 92.57, 40.60 and 11.59 for PM_{10}, $PM_{2.5}$ and PM_1, respectively. Substitution of Eq. (4) into Eq. (3) gives:

$$PMEF_i \times W = [-a \ln(x) + c]\,[U_x \times H_m] \quad (5)$$

Furthermore, the value of H_m is taken as 8.4 m, which is the maximum height of the building; the similar assumption was taken by Jamriska and Morawska (2001). Since the value of average synoptic wind speed (U_{15}) were available from at a height of 15 m above the ground level and that the PMC measurements were taken at a height of about 1.8 m (Section 3.1), we applied the log-law to predict the wind speed (U_x) at a height (z) of 1.8 m using the Eq. (6):

$$U_x = \frac{u*}{k} \ln\left(\frac{z-d}{z_0}\right) \quad (6)$$

where $u*$ (= 0.26 m s^{-1}) is surface friction velocity, k (= 0.40) is a constant, z_0 (= 0.5 m) is surface roughness length, and d (= 1 m) is the zero displacement height (Britter and Hanna, 2003). Substitution of Eq. (6) into Eq. (5) gives our final equation to estimate the PMEFs as:

$$PMEF_i = \frac{[-a \ln(x) + c] \times H_m \times \left(\frac{u*}{k} \ln\left(\frac{z-d}{z0}\right)\right)}{W} \quad (7)$$

2.5 Estimation of the respiratory deposited doses (RDD)

The mass–based RDD, based on deposition fraction (DF) values, for various PM fractions are estimated using the Eq. (8):

$$\text{RDD of PM fractions} = (\text{VT} \times f) \times \text{DF}_i \times \text{PM}_i \quad (8)$$

where DF values are estimated based on the mass median diameter (d_p) of PMCs in various size ranges (SI Figure S1) using the Eqs. (9-10) given by Hinds (1999):

$$DF = IF\ (\ 0.058 + \frac{0.911}{1+\exp(4.77+1.485\ln dp)} + \frac{0.943}{1+\exp\ (0.508-2.58\ln dp)}) \quad (9)$$

where *IF* is the inhalable fraction that is computed as:

$$IF = 1 - 0.5(1 - \frac{1}{1+0.00076\ dp^{2.8}}) \quad (10)$$

The d_p is considered as the average particle diameter by mass of the coarse and fine particle fractions, which is estimated by plotting the cumulative fraction of PMC against the particle diameter for each measurement type (SI Figure S1). VT is tidal volume that is considered equal to 1920 (1360) and 1250 (990) cm^3 per breath during heavy and light exercises for men, respectively; the values in parenthesis are for females (Hinds, 1999). *f* is the typical breathing frequency, which is taken as 0.45 (0.55) and 0.34 (0.35) breath per second during heavy and light exercises for male, respectively; the values in parenthesis are for females (Hinds, 1999). The resulting product of VT, *f* and DF to PM_{10}, $PM_{2.5}$ and PM_1 values provide mass-based RDDs.

3. RESULTS AND DISCUSSION

3.1 PMCs downwind of the demolition site

Figures 4a and 4b show the average PMCs and their fractions in various size ranges,

respectively, from the building demolition activity during the fixed–site measurements (SI Figure S2). Polar concentration rose were also plotted to identify the locations of the source during different wind directions (Figures 4c-e). These polar plots clearly showed increments in PM_{10} (Figure 4c), $PM_{2.5}$ (Figure 4d) and PM_1 (Figure 4e) when the prevailing wind was from demolition to monitoring sites. In fact, the overall average of PM_{10}, $PM_{2.5}$ and PM_1 concentrations were found to be 133.1±17.2 μg m^{-3}, 15.0±6.3 μg m^{-3} and 7.9±5.2 μg m^{-3}, with a fraction of about 89, 5 and 6% in $PM_{2.5-10}$, $PM_{1-2.5}$ and PM_1 size ranges, respectively (SI Section S3). Fraction of coarse particles (i.e. $PM_{2.5-10}$) was found to be about 39% higher over the background level, compared with fine particles (i.e. $PM_{2.5}$) that reduced by about similar percentage, against the background level during the demolition periods. This observation clearly suggests a much higher increase of coarse particle emissions from building demolition (Figure 4).

As far as the regulatory metrics are concerned, the average concentrations of PM_{10}, $PM_{2.5}$ and PM_1 were found to be up to 11-times higher during the demolition periods than the background levels of PM_{10} (12.0±6.3 μg m^{-3}), $PM_{2.5}$ (6.07±2.6 μg m^{-3}) and PM_1 (2.0±1.1 μg m^{-3}; Figure 2a). Published studies on this topic are limited for direct comparison but our results were analogous to that observed by previous studies. For example, Dorevitch et al. (2006) measured PM_{10} during the demolition of a brick-walled reinforced concrete building and average concentrations were reported to be up to 10-times higher compared with background levels. Later, Hansen et al. (2008) measured PM_1 particles from the demolition of a brick-walled concrete building and found about 3-fold increase in concentration during the demolition over the background values.

The differences in *peak* concentrations with respect to the background levels changed drastically.

For example, the *peak* values of PM_{10}, $PM_{2.5}$ and PM_1 during the demolition period increased to about 7358, 348 and 42 μg m^{-3}, which were 615–, 60– and 30–times higher than the background levels, respectively. Closer inspection of the log-sheets indicated these peak increments to be coinciding with the periods of intense breaking of the ceiling and side walls at the upper floors of the demolished building (Figure 4).

Histograms of PM_{10}, $PM_{2.5}$ and PM_1 concentration were made using the SPSS statistical software for comparing measured concentrations against the air quality standards (SI Figure S3). The EU Directive 2008/50/EC (Directive, 2008) and WHO guidelines (WHO, 2006) suggest the daily mean concentrations of PM_{10} and $PM_{2.5}$, not to exceed of 50 μg m^{-3} (on more than 35 occasions per year) and 25 μg m^{-3}, respectively. The results showed that a cumulative percentage of concentrations for about 42% exceeded the EU daily limit value for PM_{10} and about 11% of the time the daily mean WHO guideline value of $PM_{2.5}$.

The above observations clearly suggest increased considerations above the background and exceedances over the regulatory limits, especially for daily mean PM_{10}, for over 1/3rd of total demolition period. On the other hand, the exceedances of $PM_{2.5}$ were minimal, indicating that more efficient preventive measures (e.g. wind barriers, building sealing by impermeable plastic foil or water spraying (Kumar et al., 2012a) is needed to contain the PM_{10} emissions within the site boundaries in order to decrease the exposure to public in the downwind of such sites.

3.2 Spatial variations of PM during mobile measurements

In order to understand the exposure to people around the demolition site, we assessed the spatial variation of PM_{10}, $PM_{2.5}$ and PM_1 concentrations on the routes A and B that have a closed "mobile monitoring" loop of about 100 and 600 m, respectively, around the demolition site. The

average PM_{10}, $PM_{2.5}$ and PM_1 for the route A were measured as 162.7±48.4, 15.5±0.8 and 4.7±1.2 μg m^{-3} (Figure 5a), respectively, with about 4- and 2-times lower PM_{10} (37.2±9.1 μg m^{-3}) and $PM_{2.5}$ (7.5±3.6 μg m^{-3}) and slight decrease in PM_1 (3.5±1.0 μg m^{-3}) at the route B (Figure 5b). Fractions of coarse (and fine) particles were found about 90% (10%) and 79% (21%) at routes A and B, respectively (SI Figure S4). The higher PMC and fraction of coarse particles at the route A was expected, given that this route was around the periphery of the site compared with route B which was further apart from the demolition site (Table 3).

The increase in PMC during the mobile measurements cannot be directly attributed to the demolition activity since the collected data also included the periods when the mobile sampling location was in the upwind of the routes A and B. Therefore, to separate the upwind (primarily baseline, or background, PM concentrations arriving at the site) and downwind concentrations (primarily baseline plus the contribution from the building demolition), we firstly plotted the spatially averaged PM concentrations (Figure 6) and then divided the upwind and downwind data set to identify contribution from the demolition activity. For both the routes, the PMCs were much higher in downwind than those in upwind of the site and these differences were highest for the PM_{10}, followed by $PM_{2.5}$ and PM_1. For example, the average PM_{10} $PM_{2.5}$ and PM_1 in downwind (217.4, 21.0 and 6.6 μg m^{-3}) were about 7.7, 2.3 and 2.1 times higher than those in upwind (28.3, 9.3 and 3.1 μg m^{-3}) areas of the demolition site on the route A; with corresponding values on the route B being 63.6, 12.3 and 4.7 μg m^{-3} (in downwind) and 21.0, 3.1 and 2.0 μg m^{-3} (in upwind).

Peak concentrations are usually reflection of the intense emission activities, which reached to 3510.9 (PM_{10}), 244.5 ($PM_{2.5}$) and 31.2 μg m^{-3} (PM_1) which were 16.2, 11.6 and 4.7-times over

the average PMCs on the downwind of the route A. Our manual log of activities showed these peak PMCs corresponding to intense breaking of reinforced concrete beams and removal of waste material from the site that may have led to generation and resuspension of particles from the site. It was clear from the results that the close vicinity (route A) of the demolition site in downwind wind direction was significantly more influenced by PM emissions and that the most influenced size range was PM_{10}.

It will be interesting to put our measurements in the context of relevant mobile measurement studies. For example, Gulliver and Briggs (2004) reported results on variation of PM_{10} concentration during walking on the suburban routes in Northampton, UK. Their average PM_{10} concentrations (38.1±25.1 μg m^{-3}) were ~6 and 2-times lower than those found in downwind of our routes A and B, respectively. Furthermore, Kaur et al. (2005) found the average concentration of $PM_{2.5}$ to be 27.5 μg m^{-3} during the measurement of pedestrian exposure during walk along a major road in London (UK), which was slightly higher (~1.3) than our averaged downwind $PM_{2.5}$ (21.0 μg m^{-3}). Our downwind $PM_{2.5}$ on the route A were about 3-times higher than those found inside the car (6.60 μg m^{-3}) by Weichenthal et al. (2014) in Toronto (Canada). This is clear from the above contextualisation that while PM_{10} concentrations can be much higher in the downwind of demolition sites compared to those the most polluted roadside environments in urban areas; the $PM_{2.5}$ emissions from demolition are generally less pronounced and comparable to urban walking and in-vehicle studies.

3.3 Concentrations inside the excavator cabin and temporary on-site office

Excavator vehicle and on-site temporary office are integral part of demolition sites where drivers and on-site workers remain present. In order to understand how the concentration levels

364 change during the demolition periods in these settings, the measurements made showed the
365 *average* (and *peak*) concentrations of PM_{10}, $PM_{2.5}$ and PM_1 inside the excavator cabin as
366 455±349 (54124), 109±54 (12401) and 75±14 (699) μg m^{-3}, respectively (Figure 7a), which
367 were about 38- (4500-), 18- (2060-) and 37- (350-) times higher than those during the
368 background periods, respectively. These relatively higher average concentrations and the notably
369 high peak values inside the excavator cabin, compared with fixed-site (Section 3.1) and mobile
370 measurements (Section 3.2), were expected due to a very close proximity (~5 m) of the excavator
371 cabin from the demolition site.

372 As for the concentrations in on-site temporary office, the *average* (and *peak*) concentrations of
373 PM_{10}, $PM_{2.5}$ and PM_1 were measured as 90±4 (2566), 16±6 (341) and 8±4 (26) μg m^{-3} during the
374 days of measurements, respectively (Figure 7b). The corresponding *average* (and *peak*) PM_{10},
375 $PM_{2.5}$ and PM_1 increased to 8- (214-), 9- (57-) and 7- (13-) times higher over the background
376 levels during the building demolition periods. These peak values for on-site office were recorded
377 during the time of intense demolition of the building's ceiling and falling of demolished
378 materials such as brick and concrete pieces from heights to the ground level at the site.
379 Furthermore, a greater fraction of coarse particles (i.e. 83%), compared to that (~76%) in
380 excavator cabin, was found in on-site temporary office (Figure 7). The windows and doors of
381 both the temporary office and excavator cabin were closed during the measurement periods, with
382 frequent in/out movement of office workers from temporary office. Both the fixed-site (Figure
383 4b) and mobile (Figures 5a-b) measurements showed that the demolition activities produce much
384 higher fraction of coarse particles ($PM_{2.5-10}$) compared with fine particles ($PM_{2.5}$). Therefore the
385 higher ventilation in temporary office due to in/out movement of office workers could have
386 added larger fraction of coarse particles in temporary office compared with the much air tighter

387 excavator cabin.

388 The above results clearly reflect that drivers of excavator vehicle and the other on-site workers,
389 engineers or supervisors are exposed to relatively high level of PM concentrations at the
390 demolition sites. The levels of concentrations, as expected, reduce with the distance from the
391 source (i.e. demolition site in this case) and release of emissions from demolition activity is
392 much larger in PM_{10} size fraction compared with $PM_{2.5}$ (Figure 7).

393 **3.4 PM decay profiles**

394 The PM data collected at different downwind distances (i.e. at 10, 20, 40 and 80 m) was
395 plotted for evaluating the horizontal decay in concentrations of PM_{10}, $PM_{2.5}$ and PM_1 in the
396 downwind of demolition site (Figure 8). In order to find the best fit function, both the
397 logarithmic (Figure 8) and exponential (SI Figure S5) best fit functions were applied to our net
398 ΔPM_{10}, $\Delta PM_{2.5}$ and ΔPM_1 concentrations, which were determined by subtracting the background
399 PMCs from the measured concentrations during the demolition period. The ΔPM concentrations
400 at downwind distances showed a negatively correlated logarithmic form (Figure 8), with R^2
401 values as 0.94 (ΔPM_{10}), 0.93 ($\Delta PM_{2.5}$) and 0.84 (ΔPM_1). For the discussion purposes, the
402 logarithmic decay function (Figure 8) was chosen as a best fit to our data due to better R^2 values
403 than those given by an exponential decay profile as 0.85, 0.89 and 0.68 for ΔPM_{10}, $\Delta PM_{2.5}$ and
404 ΔPM_1), respectively (SI Figure S5).

405 The decay profiles suggest a higher rate of change in PM concentrations close to the demolition
406 site compared with those at farther distances. For example, the rate of change in ΔPM_{10}, $\Delta PM_{2.5}$
407 and ΔPM_1 concentration with per meter distance are (1.60, 0.51, 0.27) μg m^{-3} between 10 and 20
408 m, which decreases to (0.27, 0.45, 0.04) and (0.19, 0.06, 0.01) μg m^{-3} per meter distance in the

20-40 m, and 40-80 m range, respectively (Figure 8).. Furthermore, the average PM_{10}, $PM_{2.5}$ and PM_1 concentrations reached to half of their initial concentrations within 80, 50 and 50 m from the demolition site, respectively (Figure 8). Similar decay profiles from demolition works are not available for comparison but other studies for construction or roadside (Buonanno et al., 2009; Hagler et al., 2009; Hitchins et al., 2000) have either logarithmic or exponential decay profiles. For example, Azarmi et al. (2015b) and Buonanno et al. (2009) found the decay profiles of PM_{10} and $PM_{2.5}$ for the construction works in London (UK) and at the highway in Cassino (Italy) as logarithmic and exponential, respectively. In order to understand how far the initial concentrations from demolition site reaches to meet the standard limits, we compared the daily limits of the EU Directive 2008/50/EC (Directive, 2008) for PM_{10} and WHO guidelines for $PM_{2.5}$ (WHO, 2006) with our decaying concentrations (SI Section S4). PM_{10} and $PM_{2.5}$ took 50 and 15 m in the downwind of demolition site to meet the EU and WHO daily mean standard values, respectively (SI Figure S6). This distance could be taken as a public exclusion zone in the downwind direction of such demolition sites during demolition days.

3.5 The PMEFs for building demolition

Using the modified box model described in Section 2.4 and the PM data monitored downwind of the building demolition at the fixed-site (Section 3.1), the average PMEFs for PM_{10}, $PM_{2.5}$ and PM_1 were estimated as 35±1, 17±4 and 4±0.5 $\mu g\ m^{-2}\ s^{-1}$, respectively (SI Table S3). While there are numerous field studies available for emission factors from road traffic (Kumar et al., 2011b), limited studies are available for road works (Font et al., 2014) and almost none for building demolition activity. For example, Font et al. (2014) estimated emission factors for PM_{10} from road works in London as 0.0022 kg m^{-2} $month^{-1}$ which was about 6-fold smaller than those observed (0.013±0.004 kg m^{-2} $month^{-1}$) in our case (SI Section S5). This difference

clearly suggest much larger emissions of PM_{10} during building demolition, which is expected given its dry and intense nature compared with less intense construction activities in relatively open areas such around roads. Our results were about 19-fold higher than those reported in the UK National Atmospheric Emissions Inventory (NAEI) for the PM_{10} as 0.0007 kg m^{-2} $month^{-1}$ (NAEI, 2013) and about 2-fold greater than European emission inventory median value (0.0068 kg m^{-2} $month^{-1}$) (EMEP-EEA, 2013) for the demolition and construction activities (SI Figure S7). The PMEF of $PM_{2.5}$ and PM_1 from demolition, construction or road works are currently unavailable and hence our estimates provide hitherto missing information for future experimental and modelling studies.

3.6 Morphology and chemical characterisation

SEM and EDS analyses were performed on the bulk mass of particles collected on the filters (Table 2) for assessing their shape, size, composition and structure (SI Section S6). Figure 9 shows the SEM images of the samples, indicating a heterogeneous structure with crystal and aggregated shaped particles during the demolition works; the irregular shaped holes show the porosity of PTFE filters. EDS analysis suggested the dominance of silicon, Si (10.5-17.8%) and aluminium, Al (4.2-5.1%; Table 4). The crystal shaped particles are thought to be Si released from concrete debris (Srivastava et al., 2009) while the aggregated shaped particles shows the presence of metals such as Al (Falkovich et al., 2001). The EDS analysis also showed the presence of other elemental species (Table 4), with a strong peak for carbon (C) and fluorine (F) in the blank “reference” filter, with an additional peak of nitrogen (N) in the background sample (SI Figure S8). C and F are thought to be the material of PTFE filters while presence of N in the background filter is possibly from the regional background in a nitrate form due to secondary gas-to-particle aerosol formation (Schaap et al., 2004; Viana et al., 2008).

455 The differences between particles deposited on the reference (sample 1) and background (sample
456 2) filters and those collected during the demolition activity periods (samples 3, 4 and 5) signify
457 the presence of *new* elements (Figure 9). Apart from the dominating fraction of Si and Al, the
458 additional elements during the demolition periods were found to be sulphur (S), chlorine (Cl),
459 magnesium (Mg), sodium (Na) and Zinc (Zn), as shown in Table 4. The potential sources of
460 these elements in urban environments are summarised in SI Table S4. Some of the deposited
461 elements could be in oxide form because of presence of O during the demolition activities. The
462 increment in the intensity and ratio of O peak compared with other peaks like Si, Al and S
463 suggested that these elements appear to be strongly related with building demolition sources
464 where aluminium oxide, sulphur oxide and silicon dioxide compounds are expected to be
465 formed. The main source of Si is likely to be building related activities, particularly those
466 involving concrete material such as breaking concrete slabs, which is typically made of cement,
467 admixtures, water and aggregates (Kumar and Morawska, 2014). Si can be found in asbestos-
468 containing hazardous building materials and it is also one of the key constituents of cement in the
469 form of celite (tetracalcium aluminoferrite), belite (dicalcium silicate) and alite (tricalcium
470 silicate) (Beck et al., 2003; Lioy et al., 2002). Al were thought of coming from breaking and
471 demolition of aluminium windows, steel beams and concrete since alumina (Al_2O_3) is integral
472 component of cement (Azarmi et al., 2015b). There are sources such as sea salt and fuel oil fly
473 ash for S (SI Table S4) but this is expected to be predominantly arising from diesel exhaust
474 emissions from the construction machinery (Dorado et al., 2003). Furthermore, Na and Cl was
475 mostly likely due to the effect of sea salt brought by the south-westerly winds to the site (Figure
476 2). Zn and Mg were expected to be contributed by on-site exhaust emissions from construction
477 machinery and soil dust, respectively. The above results reflect the dominance of Si and Al in

478 particles and the ability of building demolition works to effectively aerosolise both friable and
479 non-friable building materials to the surrounding environment.

480 **3.7 Exposure to demolition workers and engineers**

481 The average RDD of coarse and fine particles were estimated using the methodology
482 described in Section 2.5 for people on and around the demolition sites (i.e. workers, individuals
483 around the demolition site, engineers inside a temporary on-site office and drivers inside the
484 excavator vehicle cabin) during heavy and light exercise levels (Table 5). Compared to the local
485 background (pre-demolition) exposure levels, the RDD of coarse and fine particles were found to
486 be 58- and 5-times in the excavator vehicle cabin, respectively, which happens to be the highest
487 exposure among all the assessed categories. This was followed by the fixed-site "downwind"
488 measurements where RDD rate for coarse (and fine) particles were 20- (and 3-) times over the
489 background, followed by 32- (and 4-) times at the downwind of mobile measurements on the
490 routes A compared to only 9- (and 3-) times at the route B and 13- (and 2-) times in the on-site
491 temporary office (Figure 10). Given a logarithmic decay of emissions away from the site
492 (Section 3.4), the distance from the demolition site was an important variable to describe the
493 differences in RDD. For example, highest RDD were calculated at the closed locations to the
494 source, such as at the excavator vehicle cabin (SI Figure S9).

495 As expected, downwind RDD of coarse (and fine) particles during mobile measurements were
496 10- (and 3-) times higher for route A, and 3- (and 4-) times higher for route B, respectively,
497 compared to those in upwind of demolition site. These downwind exposures are much higher
498 than those reported during walking on typical urban routes. For instance, we used the PM_{10} and
499 $PM_{2.5}$ concentrations measured by Gulliver and Briggs (2004) during walking on suburban routes

in Northampton, UK to calculate RDD for comparison. Their RDD for coarse (and fine) particles were found to be up to 8- (and 2-) and 2- (and 0.8-) times less than our downwind RDD during the mobile measurements at routes A and B, respectively.

Our result also showed that exposure to coarse particle is greater compared with fine particles due to the disproportionate increments in concentrations of coarse particles from demolition works (Sections 3.1-3.3). Male subjects breathe and inhale higher doses of coarse and fine particles, compared with female subjects, due to differences in body tidal volume and higher frequency of breathing (Section 2.5; Figure 10). Furthermore, given that breathing rate and frequency is higher during heavy exercises such as removing and segregating demolished materials for re-use or recycling, exposure rates could vary substantially depending on the nature of work workers are involved even if all the workers are exposed to same emission source (SI Section S7). Moreover, the results of physicochemical analysis of collected particles on the filters reflected the dominance of Si and Al (Section 3.6). Exposure to Si have been linked with variety of adverse effects such as lung (Attfield and Costello, 2004) and renal (Steenland et al., 2001) diseases; both of which have been found to result in increased rate of mortality (Calvert et al., 2003). In addition, inhaling higher doses of Al have been associated with the cardiovascular (Sjogren, 1997) and Alzheimer's (Polizzi et al., 2002) diseases, besides leading to increased morbidity, particularly in older people. It worth highlighting that the exposure doses of coarse particles indicate up to 57-times higher doses over the typical background levels for the male on-site workers during heavy or light activity (Table 5). Since Si, Al and other elements such as Mg and Zn (Table 5) are integral part of inhaled particles, there is clearly an increased health risks at demolition sites.

4. SUMMARY, CONCLUSIONS AND FUTURE WORKS

Size-resolved mass distributions of particles were measured in the 0.22–10 µm size range through a combination of measurement strategies (e.g. fixed-site and mobile). The objectives of this study were to assess emission characteristics of PM emissions in various size ranges during the mechanical demolition of a building, in addition to understand their physicochemical characteristics and the occupational exposure of workers to PM_{10}, $PM_{2.5}$ and PM_1 on and around the demolition site.

The following conclusions are drawn:

- The mass concentrations of average PM_{10}, $PM_{2.5}$ and PM_1 were found to be about 11-, 3- and 4-times above the local background levels during fixed-site measurements at the downwind of the demolition site. The coarse particles ($PM_{2.5-10}$) contributed majority (89%) of the total PMCs. The largest PM_{10}, $PM_{2.5}$ and PM_1 were detected in the excavator cabin during the demolition of building's ceiling and walls.
- The overall average PM_{10}, $PM_{2.5}$ and PM_1 during mobile measurements at route A were found to be 4-, 2- and 1.5-times higher than those at the route B (larger periphery of the site), mainly due to route A being the closed periphery of the demolition site. Segregation of the data in the downwind of the demolition site showed up to 8- and 2.5-times higher PM_{10} and $PM_{2.5}$ concentrations than those in the upwind of the mobile routes, respectively. These observations substantiate our previous findings that the demolition activities produce much larger PM_{10} emissions compared with $PM_{2.5}$. The exposure to high PMCs can be minimised by staying indoors or being positioned upwind of demolition sites.
- ΔPM_{10}, $\Delta PM_{2.5}$ and ΔPM_1 values during the demolition period in the downwind direction showed a logarithmic decay with distance ($R^2 \approx 0.90$). Such decay profiles are important for

545 extrapolating emissions in downwind of building demolition and incorporate them in
546 dispersion models such as we used in PMEF modelling. PM_{10} and $PM_{2.5}$ concentrations meet
547 the daily mean EU and WHO limit values at about 50 and 15 m, respectively, suggesting this
548 as a public exclusion zone in this particular case.

549 • Average emission factors during fixed-site monitoring of demolition activity were calculated
550 as 35.3±12.7, 12.2±3.6 and 3.9±0.5 $\mu g\ m^{-2}\ s^{-1}$ for PM_{10}, $PM_{2.5}$ and PM_1, respectively. Such
551 emission factors are currently lacking, but are key input to dispersion models for accurately
552 estimating the affected area around demolition sites and design appropriate measures to limit
553 the exposure of nearby public.

554 • SEM images indicated irregular, aggregated and crystal shaped particles during the
555 demolition works while the EDS analysis suggested the dominance of Si and Al in the
556 particles. The escape of these elements along with others such as S, Zn and Mg suggest
557 towards appropriate protection measures of population, particularly sensitive subgroups (e.g.
558 elderly and children) and those in nearby sensitive areas (e.g. hospitals, retirement home or
559 nurseries).

560 • The downwind distance from the demolition site was an important factor to dictate the
561 exposure doses. For example, highest exposure doses to coarse (and fine) particles were
562 found to be inside the excavator vehicle cabin, which were up to 6- (and 5-), 5- (and 3-) and
563 17- (and 6-) times higher than those in downwind at the fixed-site, downwind of the mobile
564 route A and temporary on-site office, respectively. Other factors affecting the exposure doses
565 of individual workers depend on their nature of work and type of physical exercise and
566 therefore the RDD rates could be different to workers involved in heavy and light exercise,
567 site engineers or drivers even if they are exposed to same level of particle concentrations.

This study focuses on PM_{10}, $PM_{2.5}$ and PM_1 generated from the demolition of a 3-storey brick-walled concrete building. The results showed effect of PM emissions on the exposure to people on and around such sites. The elevated PMCs during the demolition represent a potential health risk due to exposure to a wide variety of toxic elemental species. The results are also important for the development of mitigation strategies prior to the demolition operations and accordingly choose special protective equipment to limit exposures during the demolition activities. The male subjects inhale more doses of particles than female subjects, because of their higher body tidal volume and breathing frequency and that the rate of deposited particles could considerably increase during heavy exercises by workers for the same emission source. This suggests varying RDD rates to individual workers depending on their nature of work. The PMEFs assessed in this study can be used for developing the emission inventories while the decay profiles are important findings for estimating the dilution of particles in the downwind areas of such demolition sites. Moreover, the estimates of RDD rates are useful to compare the extent of exposures to coarse and fine particles between the demolition operations and those during exposure in typical roadside (Kumar et al., 2008, 2014) or transport microenvironments (Joodatnia et al., 2013; Goel and Kumar, 2015) in urban areas. Further personal monitoring studies, focusing on individual workers with different level of physical activities at large-scale demolition sites, are recommended to advance the understanding of occupational exposure of on-site workers. In order to provide adequate protection to the workers and population living in neighbourhood and given that demolition studies are yet limited, further studies involving monitoring of size-resolved particles from a wide variety of buildings under different urban morphology and meteorological settings are recommended.

5. ACKNOWLEDMENT

The authors thank the University of the Surrey and Cara for supporting this work, and Prof Stephen Baker and Mr Stuart Robinson for permitting us access to the demolition site. The authors also thank Prof John Watts and Mr Chris Burt of Microstructural Studies Unit at the University of Surrey for their help in SEM and EDS analysis.

6. ASSOCIATED CONTENT

Supporting Information (SI) includes Sections S1-S7, Tables S1-S4, and Figures S1-S9.

7. REFERENCES

Attfield, M.D., Costello, J., 2004. Quantitative exposure-response for silica dust and lung cancer in Vermont granite workers. American journal of industrial medicine 45, 129-138.

Authority, G.L., Councils, L., 2006. The control of dust and emissions from construction and demolition–Best Practice Guidance. Published by Greater London Authority.

Azarmi, F., Kumar, P., Marsh, D., Fuller, G.W., 2015a. Assessment of long-term impacts of PM_{10} and $PM_{2.5}$ particles from construction works on surrounding areas. Environmental Science: Processes & Impacts 18, 208-221.

Azarmi, F., Kumar, P., Mulheron, M., 2014. The exposure to coarse, fine and ultrafine particle emissions from concrete mixing, drilling and cutting activities. Journal of Hazardous Materials 279, 268-279.

Azarmi, F., Kumar, P., Mulheron, M., Colaux, J., Jeynes, C., Adhami, S., Watts, J., 2015b. Physicochemical characteristics and occupational exposure to coarse, fine and ultrafine particles during building refurbishment activities. Journal of Nanoparticle Research 17, 1-19.

Balaras, C.A., Gaglia, A.G., Georgopoulou, E., Mirasgedis, S., Sarafidis, Y., Lalas, D.P., 2007. European residential buildings and empirical assessment of the Hellenic building stock, energy consumption, emissions and potential energy savings. Building and Environment 42, 1298-1314.

617 Beck, C.M., Geyh, A., Srinivasan, A., Breysse, P.N., Eggleston, P.A., Buckley, T.J., 2003. The
618 impact of a building implosion on airborne particulate matter in an urban community.
619 Journal of the Air and Waste Management Association 53, 1256-1264.
620 Bergdahl, I., Toren, K., Eriksson, K., Hedlund, U., Nilsson, T., Flodin, R., Järvholm, B., 2004.
621 Increased mortality in COPD among construction workers exposed to inorganic dust.
622 European Respiratory Journal 23, 402-406.
623 Britter, R., Hanna, S., 2003. Flow and dispersion in urban areas. Annual Review of Fluid
624 Mechanics 35, 469-496.
625 Brook, R.D., Rajagopalan, S., Pope, C.A., Brook, J.R., Bhatnagar, A., Diez-Roux, A.V.,
626 Holguin, F., Hong, Y., Luepker, R.V., Mittleman, M.A., 2010. Particulate matter air
627 pollution and cardiovascular disease an update to the scientific statement from the
628 American Heart Association. Circulation 121, 2331-2378.
629 Buonanno, G., Lall, A., Stabile, L., 2009. Temporal size distribution and concentration of
630 particles near a major highway. Atmospheric Environment 43, 1100-1105.
631 Calvert, G.M., Rice, F.L., Boiano, J.M., Sheehy, J.W., Sanderson, W.T., 2003. Occupational
632 silica exposure and risk of various diseases: an analysis using death certificates from 27
633 states of the United States. Occupational and Environmental Medicine 60, 122-129.
634 Cavallari, J.M., Eisen, E.A., Chen, J.-C., Fang, S.C., Dobson, C.B., Schwartz, J., Christiani,
635 D.C., 2007. Night heart rate variability and particulate exposures among boilermaker
636 construction workers. Environmental Health Perspectives, 1046-1051.
637 Croteau, G.A., Guffey, S.E., Flanagan, M.E., Seixas, N.S., 2002. The effect of local exhaust
638 ventilation controls on dust exposures during concrete cutting and grinding activities.
639 American Industrial Hygiene Association Journal 63, 458-467.
640 Diapouli, E., Papamentzelopoulou, A., Chaloulakou, A., 2013. Survey of airborne particulate
641 matter concentration at a marvle processing facility workers exposure assessment. Global
642 NEST Journal 15, 204-208.
643 Directive, E., 2008. Council Directive 2008/50/EC, on ambient air quality and cleaner air for
644 Europe. Official Journal of the European Communities L151, 1-44.

645 Dorado, M.P., Ballesteros, E., Arnal, J.M., Gomez, J., Lopez, F.J., 2003. Exhaust emissions from
646 a Diesel engine fueled with transesterified waste olive oil. Fuel 82, 1311-1315.
647 Dorevitch, S., Demirtas, H., Perksy, V.W., Erdal, S., Conroy, L., Schoonover, T., Scheff, P.A.,
648 2006. Demolition of high-rise public housing increases particulate matter air pollution in
649 communities of high-risk asthmatics. Journal of the Air and Waste Management
650 Association 56, 1022-1032.
651 ECI, 2005. 40% House Report. Environmental Change Institute.
652 http://www.eci.ox.ac.uk/research/energy/40house.php [last access on 10th October 2015].
653 Eggleston, P.A., Buckley, T.J., Breysse, P.N., Wills-Karp, M., Kleeberger, S.R., Jaakkola, J.,
654 1999. The environment and asthma in US inner cities. Environmental Health Perspectives
655 107, 439.
656 EMEP-EEA., 2013. EMEP/EEA air pollutant emission inventory guidebook. Technical guidance
657 to prepare national emission inventories. Publications Office of the European Union,
658 Luxembourg (2013) http://dx.doi.org/10.2800/92722.
659 EPA., 2011. Environmental Protection Agency, AP-42, compilation of air pollutant emission
660 factors, volume 1: stationary point and area sources. (Fifth ed.), available at:
661 http://www.epa.gov/ttn/chief/ap42, [last access 12th October 2015].
662 Falkovich, A.H., Ganor, E., Levin, Z., Formenti, P., Rudich, Y., 2001. Chemical and
663 mineralogical analysis of individual mineral dust particles. Journal of Geophysical
664 Research: Atmospheres (1984–2012) 106, 18029-18036.
665 Fischer, A., Richter, K., Emmenegger, L., Künniger, T., 2005. PM_{10} emissions caused by the
666 woodworking industry in Switzerland. Holz als Rohund Werkstoff 63, 245-250.
667 Flanagan, M.E., Seixas, N., Becker, P., Takacs, B., Camp, J., 2006. Silica exposure on
668 construction sites: results of an exposure monitoring data compilation project. Journal of
669 Occupational and Environmental Hygiene 3, 144-152.
670 Font, A., Baker, T., Mudway, I.S., Purdie, E., Dunster, C., Fuller, G.W., 2014. Degradation in
671 urban air quality from construction activity and increased traffic arising from a road
672 widening scheme. Science of the Total Environment 497–498, 123-132.

673 Fuller, G.W., Green, D., 2004. The impact of local fugitive from building works and road works
674 on the assessment of the European union limit value. Atmospheric Environment 38,
675 4993-5002.
676 Goel, A., Kumar, P., 2015. Characterisation of nanoparticle emissions and exposure at traffic
677 intersections through fast–response mobile and sequential measurements. Atmospheric
678 Environment 107, 374-390.
679 Goyal, R., Kumar, P., 2013. Indoor–outdoor concentrations of particulate matter in nine
680 microenvironments of a mix-use commercial building in megacity Delhi. Air Quality,
681 Atmosphere and Health 6, 747-757.
682 Grimm, H., Eatough, D.J., 2009. Aerosol Measurement: The use of optical light scattering for the
683 determination of particulate size distribution, and particulate mass, including the semi-
684 volatile fraction. Journal of the Air and Waste Management Association 59, 101-107.
685 GroBmann, A., Hohmann, F., Wiebe, K., 2013. PortableDyme - A simplified software package
686 for econometric model building. Macroeconomic Modelling For Policy Evaluation 120,
687 pp. 33.
688 Gulliver, J., Briggs, D.J., 2004. Personal exposure to particulate air pollution in transport
689 microenvironments. Atmospheric Environment 38, 1-8.
690 Hagler, G.S.W., Baldauf, R.W., Thoma, E.D., Long, T.R., Snow, R.F., Kinsey, J.S., Oudejans,
691 L., Gullett, B.K., 2009. Ultrafine particles near a major roadway in Raleigh, North
692 Carolina: Downwind attenuation and correlation with traffic-related pollutants.
693 Atmospheric Environment 43, 1229-1234.
694 Hansen, D., Blahout, B., Benner, D., Popp, W., 2008. Environmental sampling of particulate
695 matter and fungal spores during demolition of a building on a hospital area. Journal of
696 Hospital Infection 70, 259-264.
697 Haynes, R., Savage, A., 2007. Assessment of the health impacts of particulates from the
698 redevelopment of Kings Cross. Environmental Monitoring and Assessment 130, 47-56.
699 Heal, M.R., Kumar, P., Harrison, R.M., 2012. Particles, air quality, policy and health. Chemical
700 Society Reviews 41, 6606-6630.

701 Hinds, W.C., 1999. Aerosol Technology: properties, behaviour and measurement of airborne
702 particles. John Wiley & Sons,USA, Second Edition, pp. 483.
703 Hitchins, J., Morawska, L., Wolff, R., Gilbert, D., 2000. Concentrations of submicrometre
704 particles from vehicle emissions near a major road. Atmospheric Environment 34, 51-59.
705 Ho, K., Lee, S., Chow, J.C., Watson, J.G., 2003. Characterization of PM_{10} and $PM_{2.5}$ source
706 profiles for fugitive dust in Hong Kong. Atmospheric Environment 37, 1023-1032.
707 HSE, 2006. Construction (Design and Management) Regulations, Health and Safety Excutive.
708 http://www.hse.gov.uk/construction/cdm/2015/legal.htm [last access on 10th September
709 2015].
710 HSE, 2011. Health and Safety Executive, Control of Substances Hazardous to Health (COSHH).
711 Essentials Guidance Publications http://www.hse.gov.uk/pubns/guidance/index.htm [last
712 access on 10th October 2015].
713 Jaecker-Voirol, A., Pelt, P., 2000. PM_{10} emission inventory in Ile de France for transport and
714 industrial sources: PM_{10} re-suspension, a key factor for air quality. Environmental
715 Modelling & Software 15, 575-581.
716 Jamriska, M., Morawska, L., 2001. A model for determination of motor vehicle emission factors
717 from on-road measurements with a focus on submicrometer particles. Science of the
718 Total Environment 264, 241-255.
719 Janssen, N.A.H., Fischer, P., Marra, M., Ameling, C., Cassee, F.R., 2013. Short-term effects of
720 $PM_{2.5}$, PM_{10} and $PM_{2.5–10}$ on daily mortality in the Netherlands. Science of the Total
721 Environment 463–464, 20-26.
722 JEOL, 2015. JSM-7100F Schottky Field Emission Scanning Electron Microscope. JEOL Ltd
723 Japan. http://www.jeol.co.jp/en/products/detail/JSM-7100F.html, [last access 14th
724 October 2015].
725 Joodatnia, P., Kumar, P., Robins, A., 2013a. The behaviour of traffic produced nanoparticles in a
726 car cabin and resulting exposure rates. Atmospheric Environment 65, 40-51.
727 Joseph, J., Patil, R.S., Gupta, S.K., 2009. Estimation of air pollutant emission loads from
728 construction and operational activities of a port and harbour in Mumbai, India.
729 Environmental Monitoring and Assessment 159, 85-98.

730 Kan, H., London, S.J., Chen, G., Zhang, Y., Song, G., Zhao, N., Jiang, L., Chen, B., 2007.
731 Differentiating the effects of fine and coarse particles on daily mortality in Shanghai,
732 China. Environment International 33, 376-384.
733 Kaur, S., Nieuwenhuijsen, M., Colvile, R., 2005. Personal exposure of street canyon intersection
734 users to $PM_{2.5}$, ultrafine particle counts and carbon monoxide in Central London, UK.
735 Atmospheric Environment 39, 3629-3641.
736 Kean, A.J., Sawyer, R.F., Harley, R.A., 2000. A Fuel-Based Assessment of off-Road diesel
737 engine emissions. Journal of the Air and Waste Management Association 50, 1929-1939.
738 Kumar, P., Fennell, P., Britter, R., 2008. Effect of wind direction and speed on the dispersion of
739 nucleation and accumulation mode particles in an urban street canyon. Science of the
740 Total Environment 402, 82-94.
741 Kumar, P., Gurjar, B.R., Nagpure, A.S., Harrison, R.M., 2011a. Preliminary estimates of
742 nanoparticle number emissions from road vehicles in megacity Delhi and associated
743 health impacts. Environmental Science & Technology 45, 5514-5521.
744 Kumar, P., Ketzel, M., Vardoulakis, S., Pirjola, L., Britter, R., 2011b. Dynamics and dispersion
745 modelling of nanoparticles from road traffic in the urban atmospheric environment-A
746 review. Journal of Aerosol Science 42, 580-603.
747 Kumar, P., Mulheron, M., Fisher, B., Harrison, R.M., 2012a. New Directions: Airborne ultrafine
748 particle dust from building activities– A source in need of quantification. Atmospheric
749 Environment 56, 262-264.
750 Kumar, P., Mulheron, M., Som, C., 2012b. Release of ultrafine particles from three simulated
751 building processes. Journal of Nanoparticle Research 14, 1-14.
752 Kumar, P., Jain, S., Gurjar, B., Sharma, P., Khare, M., Morawska, L., Britter, R., 2013a. New
753 Directions: Can a “blue sky” return to Indian megacities?. Atmospheric Environment 71,
754 198-201.
755 Kumar, P., Pirjola, L., Ketzel, M., Harrison, R.M., 2013b. Nanoparticle emissions from 11 non-
756 vehicle exhaust sources– A review. Atmospheric Environment 67, 252-277.

Kumar, P., Morawska, L., Birmili, W., Paasonen, P., Hu, M., Kulmala, M., Harrison, R.M., Norford, L., Britter, R., 2014. Ultrafine particles in cities. Environment International 66, 1-10.

Kumar, P., Morawska, L., 2014. Recycling Concrete: an undiscovered source of ultrafine particles. Atmospheric Environment 90, 51-58.

Kumar, P., Martani, C., Morawska, L., Norford L.K., Choudhary R., Leach, M., 2016. Indoor air quality and energy management through real-time sensing in commercial buildings. Energy and Buildings 111, 145-153.

Kupiainen, K., Tervahattu, H., Räisänen, M., 2003. Experimental studies about the impact of traction sand on urban road dust composition. Science of the Total Environment 308, 175-184.

Lawson, N., Douglas, I., Garvin, S., McGrath, C., Manning, D., Vetterlein, J., 2001. Recycling construction and demolition wastes-a UK perspective. Environmental Management and Health 12, 146-157.

Lim, J.M., Lee, J.H., Moon, J.H., Chung, Y.S., Kim, K.H., 2010. Source apportionment of PM_{10} at a small industrial area using Positive Matrix Factorization. Atmospheric Research 95, 88-100.

Lioy, P.J., Weisel, C.P., Millette, J.R., Eisenreich, S., Vallero, D., Offenberg, J., Buckley, B., Turpin, B., Zhong, M., Cohen, M.D., Prophete, C., Yang, I., Stiles, R., Chee, G., Johnson, W., Porcja, R., Alimokhtari, S., Hale, R.C., Weschler, C., Chen, L.C., 2002. Characterization of the dust/smoke aerosol that settled east of the World Trade Center (WTC) in lower Manhattan after the collapse of the WTC 11 September 2001. Environmental Health Perspectives 110, 703-714.

Lo, I.M.C., Tang, C.I., Li, X.-D., Poon, C.S., 2000. Leaching and microstructural analysis of cement-based solidified wastes. Environmental Science & Technology 34, 5038-5042.

Mouzourides, P., Kumar, P., Marina Neophytou, K.A., 2015. Assessment of long-term measurements of particulate matter and gaseous pollutants in South-East Mediterranean. Atmospheric Environment 107, 148-165.

785 Muleski, G.E., Cowherd Jr, C., Kinsey, J.S., 2005. Particulate emissions from construction
786 activities. Journal of the Air and Waste Management Association 55, 772-783.
787 NAEI, 2013. National Atmospheric Emissions Inventory, http://naei.defra.gov.uk/data/ef-all
788 [last access on 10th October 2015].
789 Namdeo, A., Bell, M.C., 2005. Characteristics and health implications of fine and coarse
790 particulates at roadside, urban background and rural sites in UK. Environment
791 International 31, 565-573.
792 Paoletti, L., De Berardis, B., Diociaiuti, M., 2002. Physico-chemical characterisation of the
793 inhalable particulate matter (PM_{10}) in an urban area: an analysis of the seasonal trend.
794 Science of the Total Environment 292, 265-275.
795 Peng, R.D., Chang, H.H., Bell, M.L., McDermott, A., Zeger, S.L., Samet, J.M., Dominici, F.,
796 2008. Coarse particulate matter air pollution and hospital admissions for cardiovascular
797 and respiratory diseases among Medicare patients. Journal of the American Medical
798 Association 299, 2172-2179.
799 Polizzi, S., Pira, E., Ferrara, M., Bugiani, M., Papaleo, A., Albera, R., Palmi, S., 2002.
800 Neurotoxic effects of aluminium among foundry workers and Alzheimer's disease.
801 Neurotoxicology 23, 761-774.
802 Rao, A., Jha, K.N., Misra, S., 2007. Use of aggregates from recycled construction and demolition
803 waste in concrete. Resources, Conservation and Recycling 50, 71-81.
804 Roberts, S., 2008. Altering existing buildings in the UK. Energy Policy 36, 4482-4486.
805 Rodriguez, S., Querol, X., Alastuey, A., Viana, M.a.-M., Alarcon, M., Mantilla, E., Ruiz, C.R.,
806 2004. Comparative PM_{10}–$PM_{2.5}$ source contribution study at rural, urban and industrial
807 sites during PM episodes in Eastern Spain. Science of the Total Environment 328, 95-
808 113.
809 Saliba, N., El Jam, F., El Tayar, G., Obeid, W., Roumie, M., 2010. Origin and variability of
810 particulate matter (PM_{10} and $PM_{2.5}$) mass concentrations over an Eastern Mediterranean
811 city. Atmospheric Research 97, 106-114.

812 Schaap, M., van Loon, M., ten Brink, H.M., Dentener, F.J., Builtjes, P.J.H., 2004. Secondary
813 inorganic aerosol simulations for Europe with special attention to nitrate. Atmospheric
814 Chemistry and Physics 4, 857-874.
815 Senlin, L., Zhenkun, Y., Xiaohui, C., Minghong, W., Guoying, S., Jiamo, F., Paul, D., 2008. The
816 relationship between physicochemical characterization and the potential toxicity of fine
817 particulates ($PM_{2.5}$) in Shanghai atmosphere. Atmospheric Environment 42, 7205-7214.
818 Sjogren, B., Fossum, T., Lindh, T., Weiner, J., 2002. Welding and ischemic heart disease.
819 International Journal of Occupational and Environmental Health 8, 309-311.
820 Sjogren, B., 1997. Occupational exposure to dust: inflammation and ischaemic heart disease.
821 Occupational and Environmental Medicine 54, 466-469.
822 Spencer-Hwang, R., Knutsen, S.F., Soret, S., Ghamsary, M., Beeson, W.L., Oda, K., Shavlik, D.,
823 Jaipaul, N., 2011. Ambient air pollutants and risk of fatal coronary heart disease among
824 kidney transplant recipients. American Journal of Kidney Diseases 58, 608-616.
825 Srivastava, A., Jain, V., Srivastava, A., 2009. SEM-EDX analysis of various sizes aerosols in
826 Delhi India. Environmental Monitoring and Assessment 150, 405-416.
827 Steenland, K., Sanderson, W., Calvert, G.M., 2001. Kidney disease and arthritis in a cohort study
828 of workers exposed to silica. Epidemiology, 12, 405-412.
829 Stern, F., Lehman, E., Ruder, A., 2001. Mortality among unionized construction plasterers and
830 cement masons. American Journal of Industrial Medicine 39, 373-388.
831 Tian, G., Fan, S., Li, G., Qin, J., 2007. Characteristics of fugitive dust emission from paved road
832 near construction activities. Journal of Huanjing Kexue 28, 2626-2629.
833 Toledo, V.E., de Almeida Junior, P.B., Quiterio, S.L., Arbilla, G., Moreira, A., Escaleira, V.,
834 Moreira, J.C., 2008. Evaluation of levels, sources and distribution of toxic elements in
835 PM_{10} in a suburban industrial region, Rio de Janeiro, Brazil. Environmental Monitoring
836 and Assessment 139, 49-59.
837 Turner, M.C., Krewski, D., Pope, C.A., Chen, Y., Gapstur, S.M., Thun, M.J., 2011. Long-term
838 ambient fine particulate matter air pollution and lung cancer in a large cohort of never-
839 smokers. American Journal of Respiratory and Critical Care Medicine 184, 1374-1381.

840 Verma, D.K., Kurtz, L.A., Sahai, D., Finkelstein, M.M., 2003. Current chemical exposures
841 among Ontario construction workers. Applied Occupational and Environmental Hygiene
842 18, 1031-1047.
843 Viana, M., Kuhlbusch, T., Querol, X., Alastuey, A., Harrison, R., Hopke, P., Winiwarter, W.,
844 Vallius, M., Szidat, S., Prevot, A., 2008. Source apportionment of particulate matter in
845 Europe: a review of methods and results. Journal of Aerosol Science 39, 827-849.
846 Vineis, P., Forastiere, F., Hoek, G., Lipsett, M., 2004. Outdoor air pollution and lung cancer:
847 Recent epidemiologic evidence. International Journal of Cancer 111, 647-652.
848 Weichenthal, S., Van Ryswyk, K., Kulka, R., Sun, L., Wallace, L., Joseph, L., 2014. In-vehicle
849 exposures to particulate air pollution in Canadian metropolitan areas: The urban
850 transportation exposure study. Environmental Science & Technology 49, 597-605.
851 Weng, C.H., Hu, C.C., Yen, T.H., Huang, W.H., 2015. Association between environmental
852 particulate matter and arterial stiffness in patients undergoing hemodialysis. BMC
853 Cardiovascular Disorders 15, 115.
854 WHO, 2006. Air quality guidelines: global update 2005: particulate matter, ozone, nitrogen
855 dioxide, and sulfur dioxide. World Health Organization. Available at:
856 http://www.euro.who.int/document/e90038.pdf.
857 Woskie, S.R., Kalil, A., Bello, D., Virji, M.A., 2002. Exposures to quartz, diesel, dust, and
858 welding fumes during heavy and highway construction. American Industrial Hygiene
859 Association Journal 63, 447-457.

List of Figure Captions

Figure 1. Schematic diagram of the experimental set-up, showing (a, b) monitoring stations around the demolition site (DS) during (c) fixed site measurements at day 2, and (d) day 3. Route of mobile measurements around the DS during (e) day 4, and (f) day 5. Sequential measurements of PM at the downwind of DS during (g) day 6, and (h) day 7. Solid triangles in each sub-figure show the sampling station. SP and EP refer to the start and end points, respectively, while the arrows represent the path of mobile measurements. Please note that the figure is not to scale and distances are presented in Table 1.

Figure 2. Wind rose diagrams depict the hourly frequency distribution of the wind speed and direction during the fixed-site measurement on (a) day 2, and (b) day 3, as well as during the mobile measurements on (c) day 4, and (d) day 5, together with measurements at sequential distances on (e) day 6, and (f) day 7. Please note that the unit for mean wind speed is metre per second.

Figure 3. Schematic diagram of the box model, showing various dimensions and parameters; f_x and f_z refer to the particulate mass flow rate entering and leaving the box in the x and z directions. U_x and U_z refer to wind velocities in the x and z directions; L and W refer to length and width of the box, respectively, and H_m refers to maximum mixing height.

Figure 4. (a) The average concentrations of PM_{10}, $PM_{2.5}$ and PM_1 with average of prevailing wind direction, during all days of fixed site measurements. The inner and outer circles represent fractions of PMCs in various size ranges during the background and activity periods, respectively. The polar plots show variation in concentration with the wind direction and speed and their corresponding hourly mean (b) PM_{10}, (c) $PM_{2.5}$ and (d) PM_1 concentrations, along with

882 (e) temporal profiles.

883 **Figure 5**. The average concentrations of PM_{10}, $PM_{2.5}$ and PM_1 at (a) route A and (b) route B,
884 during all days of mobile measurements. The inner and outer circles represent fractions of PMCs
885 in various size ranges during the background and activity periods, respectively. The box and
886 whiskers plots at (c) route A and at (d) route B are showing upper, middle, and lower lines of
887 "boxes" indicated 75^{th}, 50^{th}, and 25^{th} percentiles of PM_{10}, $PM_{2.5}$ and PM_1 during the building
888 demolition periods at the demolition site. Please note that SP and EP refer to the start and end
889 points, respectively.

890 **Figure 6.** The spatially averaged concentrations of PM_{10}, $PM_{2.5}$ and PM_1 during mobile
891 measurements at (a) route A and (b) route B. The words Avg, DW and UW in the figure represent
892 average, downwind and upwind, respectively. Blue triangles represent different waypoints on the
893 routes A and B between the starting and end points. Each coloured point represents the average
894 concentrations over the 12 runs each at both the routes A and B. A number of parallel points at
895 each route were due to the sensitivity of GPS device, which varied within ±3.5 m at the same
896 route. Please note that SP and EP refer to the start and end points, respectively. $PM_{2.5\text{-}10}$ (%),
897 $PM_{1\text{-}2.5}$ (%) and PM_1 (%) represent fraction of 2.5-10 µm, 1-2.5 µm, 1 µm from the total PM_{10}
898 concentrations in upwind and downwind direction on the mobile route, respectively.

899 **Figure 7**. The concentrations of PM_{10}, $PM_{2.5}$ and PM_1, at (a) the excavator cabin and (b)
900 temporary on-site office for site engineers and managers during days of measurements. The inner
901 and outer circles represent fractions of PMCs in various size ranges during the background and
902 working periods, respectively.

903 **Figure 8**. (a) Horizontal decay profiles of ΔPM_{10}, (b) $\Delta PM_{2.5}$ and (c) ΔPM_1 at the demolition site

during the sequential measurements; *x* and *y* expresses distance from the demolition site and ΔPM values, respectively. The solid line in represents the best fitting linear decay curve and the dotted line represents 50% drop from the initial concentrations.

Figure 9. SEM images of the surface morphology of the particles collected on blank filter, background measurements, sample 3, sample 4 and sample 5 at ×50, ×1000 and ×8000 resolution.

Figure 10. Factor of increased exposure (FIE) representing a ratio of respiratory deposition doses during the activities over the background level in coarse and fine particles range during each activity; deposited fractions were estimated based on mass median diameters as explained in Section 2.5.

914 # List of Tables

915 **Table 1.** Description of sampling duration and monitoring sites.

Day number	Date	Start-end time (sampling duration in minutes)	Measurement type	Measurement location with respect to demolition site (x)
1	28 June 2015	10:00:00–14:00:00 (~220)	Background	At 15 m downwind of demolition site
2, 3	1, 3 July 2015	08:56:01–17:00:07 (~500) 08:33:01–16:56:37 (~500)	Fixed-site	At 10 m downwind of the demolition site
4, 5	6, 8 July 2015	08:46:01–17:01:13 (~500) 08:35:01–16:59:25 (~500)	Mobile measurements	Around the demolition site in ~100 m (route A) and ~600 m (route B) loop
6, 7	9, 10 July 2015	14:12:01–16:46:43 (~150) 08:39:01–16:44:01 (~500)	Sequential measurements	At 10, 20, 40 and 80 m downwind of demolition site
7	10 July 2015	11:03:00–14:40:00 (~220)	Excavator cabin	At 5 m downwind inside the vehicle cabin
2, 3, 4, 6, 7	1, 3, 6, 9, 10 July 2015	15:10:00–15:49:00 (~40) 13:25:00–14:00:00 (~35) 14:30:00–15:00:00 (~30) 14:10:00–14:40:00 (~30) 15:00:00–15:10:00 (~10)	Engineer's on-site office	At 16 m downwind inside the office

916

917 **Table 2.** Summary of samples collected on PTFE filters during the demolition activity.

Name	Date of sampling	Time for sampling (min^{-1})	Mass of particles collected on the filter per unit area ($\mu g\ cm^{-2}$)[a]
Sample 1	Blank (reference)	-	-
Sample 2	28 June 2015	240	0.3
Sample 3	1 and 3 July 2015	1000	19.5
Sample 4	6 and 8 July 2015	1000	14.7
Sample 5	9 and 10 July 2015	650	16.1

918 [a]The mass of collected particles on the filter per unit area ($\mu g\ cm^{-2}$) has been calculated by
919 dividing the collected mass over the area of a filter (~17.3 cm^2).

920 **Table 3.** PM_{10}, $PM_{2.5}$ and PM_1 concentrations ($\mu g\ m^{-3}$) during mobile measurements at routes A and
921 B.

Route A				Route B			
	PM_{10}	$PM_{2.5}$	PM_1		PM_{10}	$PM_{2.5}$	PM_1
Run 1A	48.8±20.7	12.2±2.1	4.3±0.6	Run 1B	35.0±5.1	12.2±0.5	4.7±0.4
Run 2A	29.6±2.7	9.8±0.1	3.9±0.2	Run 2B	28.4±7.8	9.1±1.3	3.9±0.7
Run 3A	133.9±83.5	19.4±5.3	8.3±1.3	Run 3B	61.7±56.8	12.2±5.2	4.9±1.2
Run 4A	202.4±198.0	19.9±12.1	5.8±1.3	Run 4B	32.9±9.6	9.3±1.6	4.5±1.1
Run 5A	331.7±204.1	27.0±9.3	6.7±1.0	Run 5B	75.8±81.3	10.5±6.3	3.5±1.7
Run 6A	24.4±6.6	8.3±1.6	4.2±1.3	Run 6B	28.2±20.4	7.4±1.1	4.0±0.9
Run 7A	53.3±37.1	7.0±4.5	2.2±0.4	Run 7B	23.5±11.6	4.6±0.7	2.7±0.8
Run 8A	440.1±358.5	30.9±24.3	5.2±2.2	Run 8B	29.9±37.6	5.0±1.2	3.1±0.4
Run 9A	171.4±96.8	13.5±4.5	4.1±0.6	Run 9B	25.3±15.6	5.5±0.4	3.2±0.6
Run 10A	155.5±91.7	12.9±1.9	4.4±0.9	Run 10B	58.2±54.5	6.4±3.2	2.7±0.6
Run 11A	150.8±56.8	11.4±1.7	3.5±0.3	Run 11B	29.5±22.9	5.1±1.2	3.0±0.4
Run 12A	210.8±114.4	13.8±4.7	3.4±0.8	Run 12B	17.9±8.7	3.3±0.4	2.2±0.2
Overall average	162.7±48.44	15.5±0.8	4.7±1.2	Total	37.2±9.1	7.5±3.6	3.5±1.0

922

923 **Table 4.** The elemental composition of the all the filters (quantitative EDS analyses).

Sample 1 (Reference)		Sample 2 (Background)		Sample 3 (Fixed site)		Sample 4 (Mobile measurements)		Sample 5 (Different distances)	
Name	Fraction (%)	Name	Fraction (%)	Name	Fraction (%)	Name	Fraction (%)	Name	Fraction (%)
C	30.6	C	46.2	C	16.7	C	19.3	C	21.0
-	-	O	24.3	O	48.5	O	48.9	O	22.9
F	69.3	-	-	F	3.5	F	1.4	F	40.8
-	-	-	-	Si	17.8	Si	14.0	Si	10.5
-	-	S	1.2	S	2.3	S	4.2	-	-
-	-	-	-	Al	5.1	Al	4.5	Al	4.2
-	-	-	-	Mg	1.4	Mg	2.6	Mg	0.3
-	-	Cl	4.4	Cl	1.9	Cl	1.5	-	-
-	-	Na	2.6	Na	2.5	-	-	-	-
-	-	N	21.0	-	-	-	-	-	-
-	-	-	-	-	-	Zn	3.1	-	-

924

925 **Table 5.** The RDD rates of coarse and fine particles.

Location	Gender	Exercise level	Total RDD (μg min^{-1}×10^{-2}) ±STD		926 927 928
			Coarse particles	Fine particles	
Construction site (fixed site)	Male	Heavy	572.8±52.7	34.7±14.6	
		Light	290.0±26.6	17.5±7.4	
Around the construction site (route A)	Male	Heavy	956.0±231.8	64.8±2.5	
		Light	484.1±117.3	32.8±1.2	
	Female	Heavy	827.6±200.6	56.1±2.2	
		Light	383.4±92.9	26.0±1.0	
Around the construction site (route B)	Male	Heavy	249.7±26.8	38.0±11.2	
		Light	126.4±13.5	19.2±5.6	
	Female	Heavy	216.1±23.2	32.9±9.7	
		Light	100.1±10.7	15.2±4.5	
At different distances from the construction site (10 m)	Male	Heavy	238.7±4.7	39.5±26.9	
		Light	120.8±2.4	20.2±13.6	
	Female	Heavy	206.6±4.1	34.2±23.3	
		Light	95.7±1.9	15.8±10.8	
At different distances from the construction site (20 m)	Male	Heavy	185.1±34.4	32.0±22.4	
		Light	93.7±17.4	16.2±11.3	
	Female	Heavy	160.3±29.8	27.7±19.4	
		Light	74.2±13.8	12.8±8.9	
At different distances from the construction site (40 m)	Male	Heavy	202.9±84.0	18.7±4.7	
		Light	102.7±42.5	9.5±2.3	
	Female	Heavy	175.3±72.7	16.2±4.0	
		Light	81.3±33.6	7.5±1.8	
At different distances from the construction site (80 m)	Male	Heavy	175.5±60.3	15.4±4.1	
		Light	88.8±30.5	7.8±2.0	
	Female	Heavy	151.9±52.2	13.3±3.5	
		Light	70.4±24.1	6.1±1.6	
Inside the excavator cabin	Male	Heavy	1662.8±1422.3	78.3±38.2	
		Light	842.0±720.2	39.6±19.3	
Inside the container office	Male	Heavy	365.4±184.3	30.7±10.9	
		Light	185.0±93.3	15.5±5.5	
	Female	Heavy	316.3±159.5	26.5±9.4	
		Light	146.5±73.9	12.3±4.3	
Background	Male	Heavy	29.3±17.7	15.2±6.8	
		Light	14.8±8.9	7.7±3.4	
	Female	Heavy	25.3±15.3	13.1±5.9	
		Light	11.7±7.1	6.1±2.7	

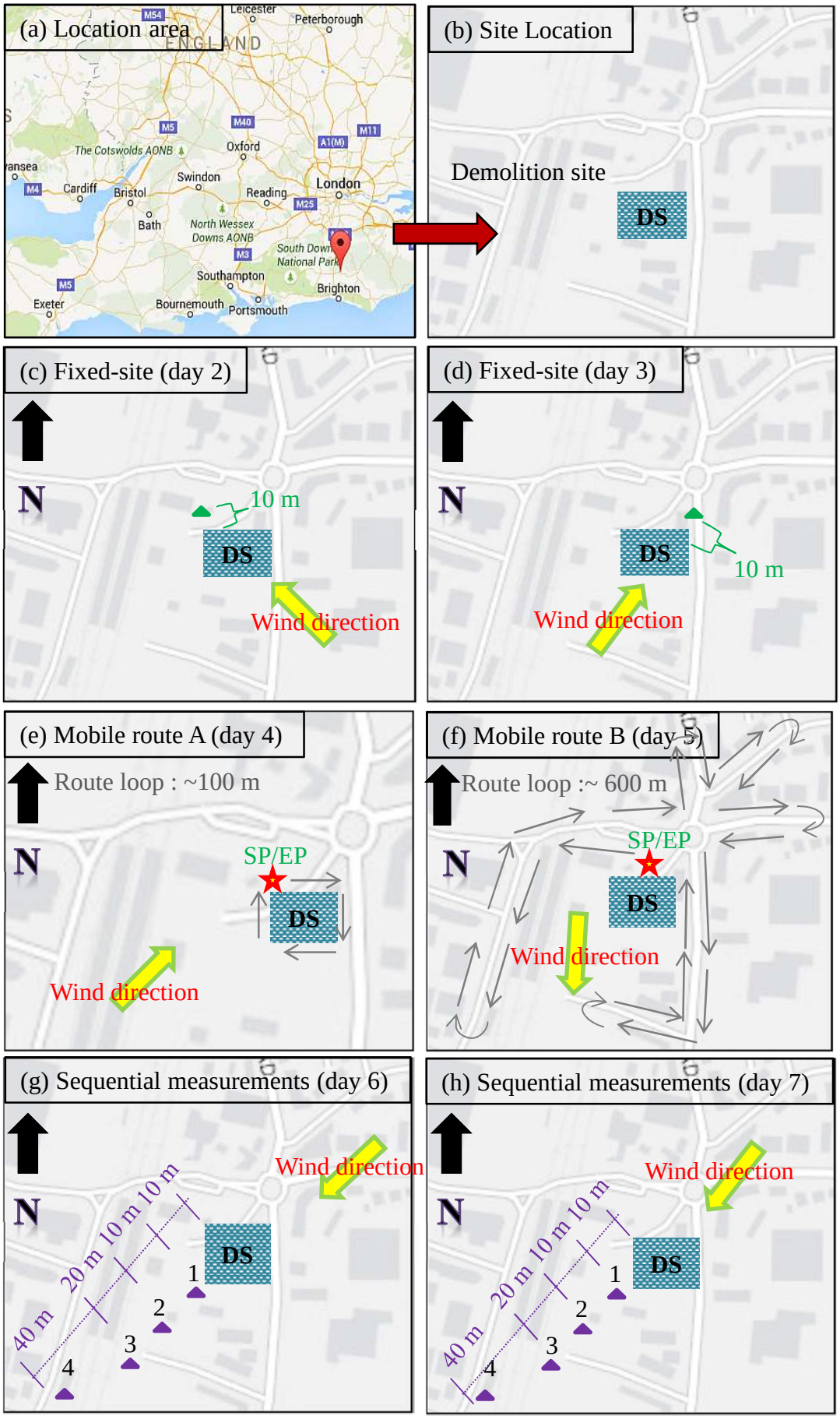
(a) Location area
Leicester
Peterborough
ENGLAND
M54
M5
M40
M11
A1(M)
The Cotswolds AONB
Oxford
Swindon
Cardiff
Bristol
Reading
London
M4
M25
Bath
North Wessex Downs AONB
M3
South Downs National Park
Southampton
Brighton
M5
Exeter
Bournemouth
Portsmouth
(b) Site Location
Demolition site
DS
(c) Fixed-site (day 2)
N
10 m
DS
Wind direction
(d) Fixed-site (day 3)
N
DS
10 m
Wind direction
(e) Mobile route A (day 4)
Route loop : ~100 m
N
SP/EP
DS
Wind direction
(f) Mobile route B (day 5)
Route loop :~ 600 m
N
SP/EP
DS
Wind direction
(g) Sequential measurements (day 6)
Wind direction
N
DS
40 m
20 m
10 m
10 m
1
2
3
4
(h) Sequential measurements (day 7)
Wind direction
N
DS
40 m
20 m
10 m
10 m
1
2
3
4

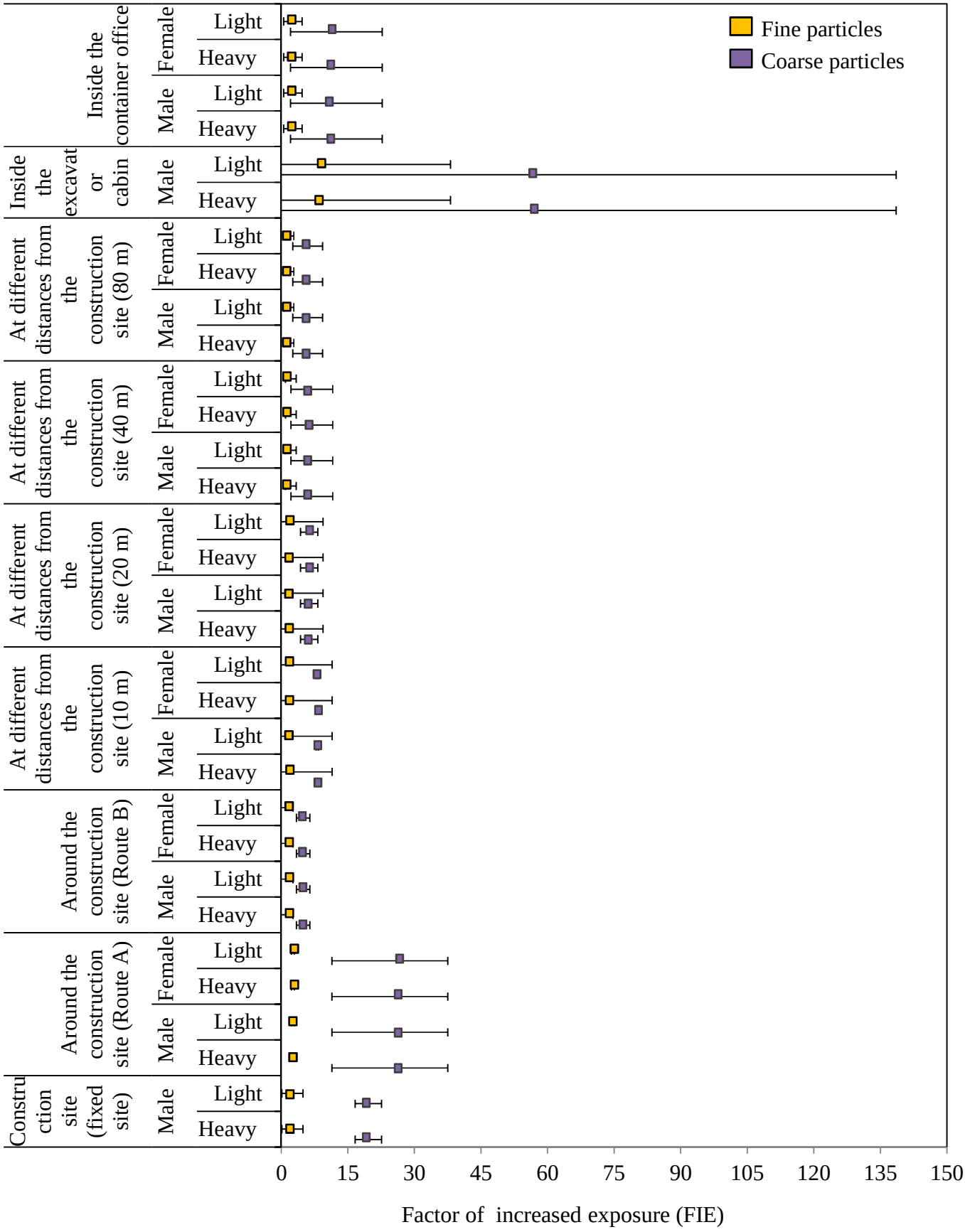
Fine particles
Coarse particles
Inside the container office
Female
Male
Light
Heavy
Inside the excavator cabin
At different distances from the construction site (80 m)
At different distances from the construction site (40 m)
At different distances from the construction site (20 m)
At different distances from the construction site (10 m)
Around the construction site (Route B)
Around the construction site (Route A)
Construction site (fixed site)
0
15
30
45
60
75
90
105
120
135
150
Factor of increased exposure (FIE)

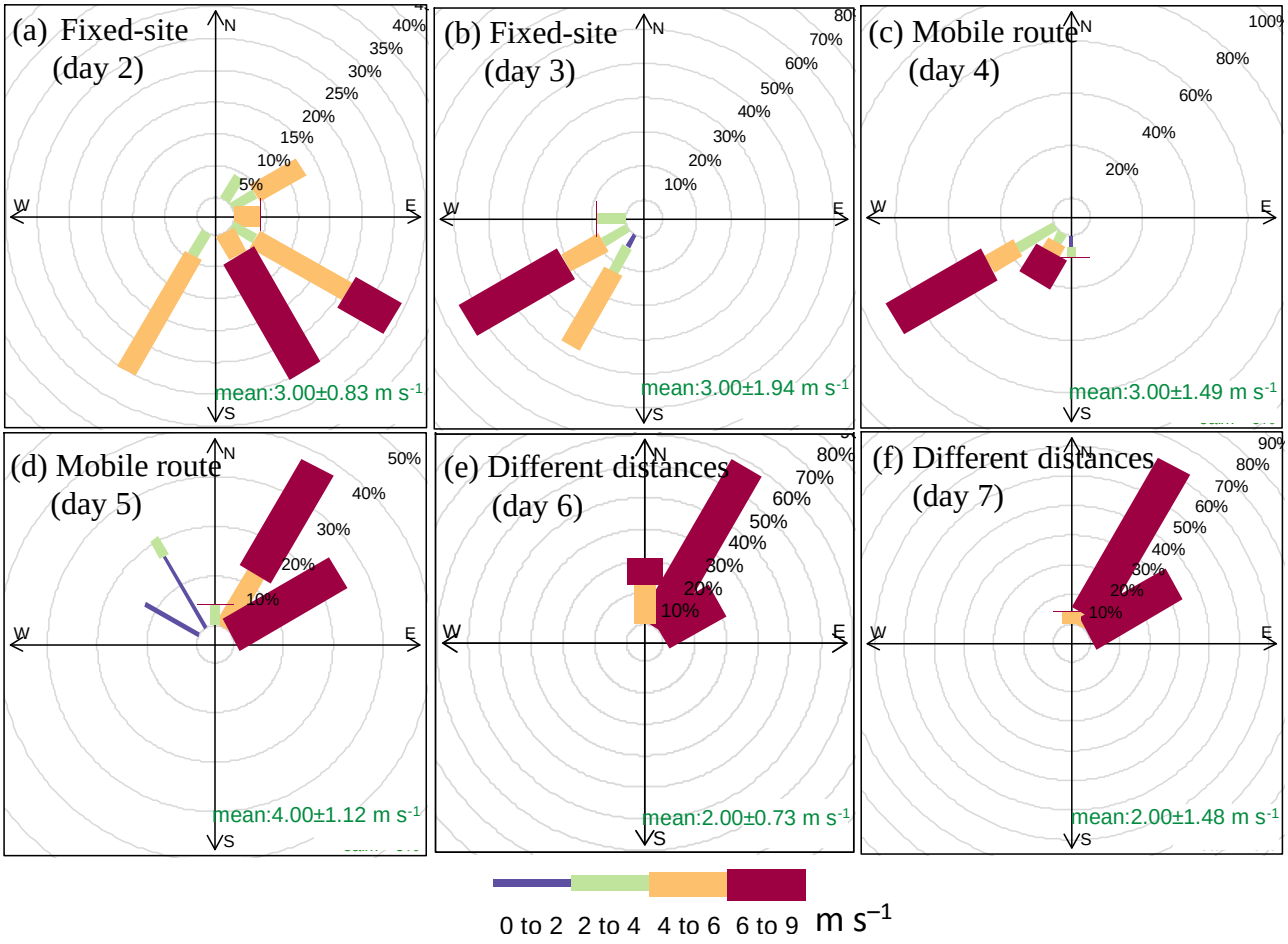
(a) Fixed-site (day 2)
mean:3.00±0.83 m s-1
(b) Fixed-site (day 3)
mean:3.00±1.94 m s-1
(c) Mobile route (day 4)
mean:3.00±1.49 m s-1
(d) Mobile route (day 5)
mean:4.00±1.12 m s-1
(e) Different distances (day 6)
mean:2.00±0.73 m s-1
(f) Different distances (day 7)
mean:2.00±1.48 m s-1
N
S
W
E
0 to 2
2 to 4
4 to 6
6 to 9
m s−1

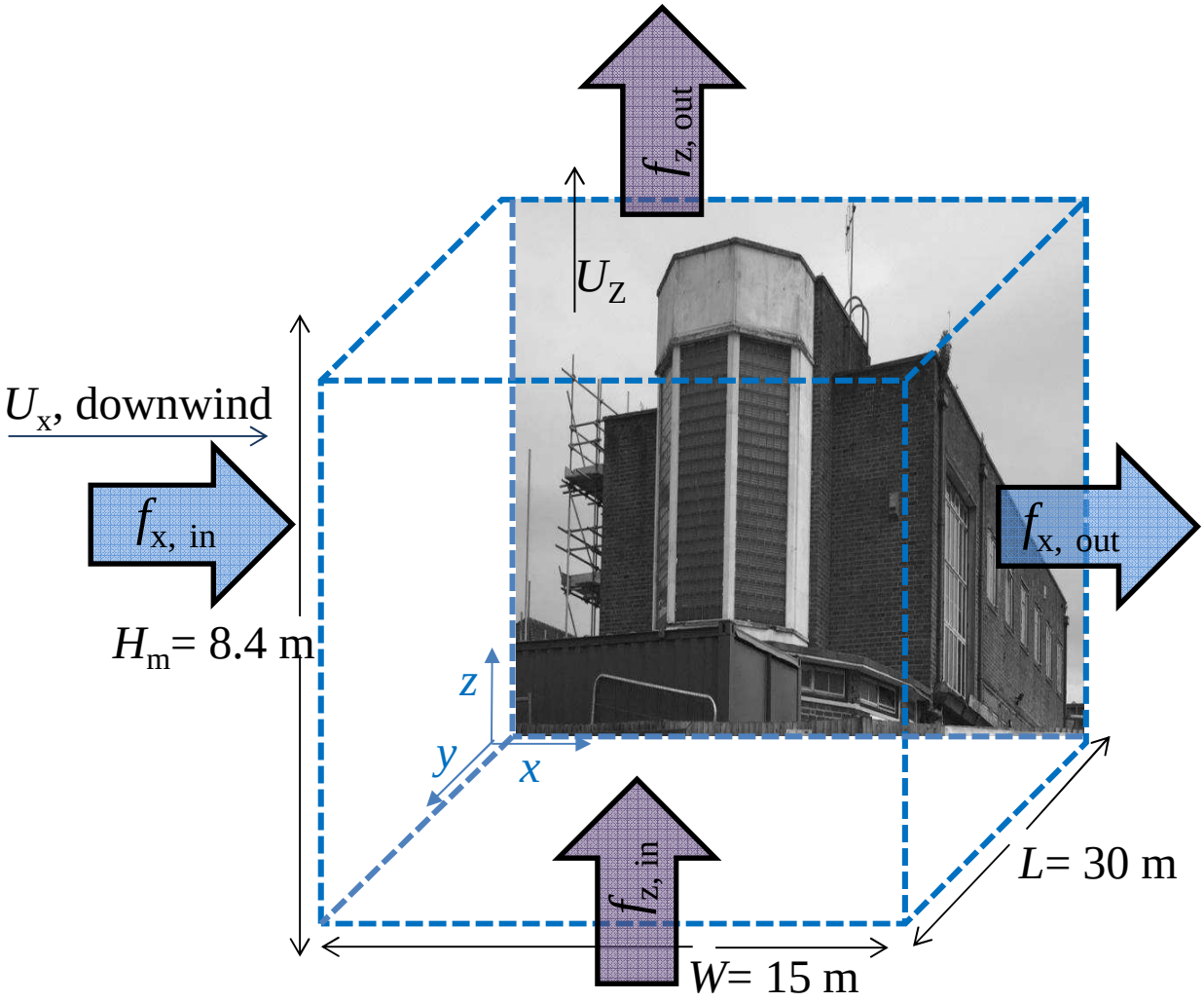
$f_{z,\,out}$
U_z
U_x, downwind
$f_{x,\,in}$
$f_{x,\,out}$
H_m= 8.4 m
z
y
x
$f_{z,\,in}$
L= 30 m
W= 15 m

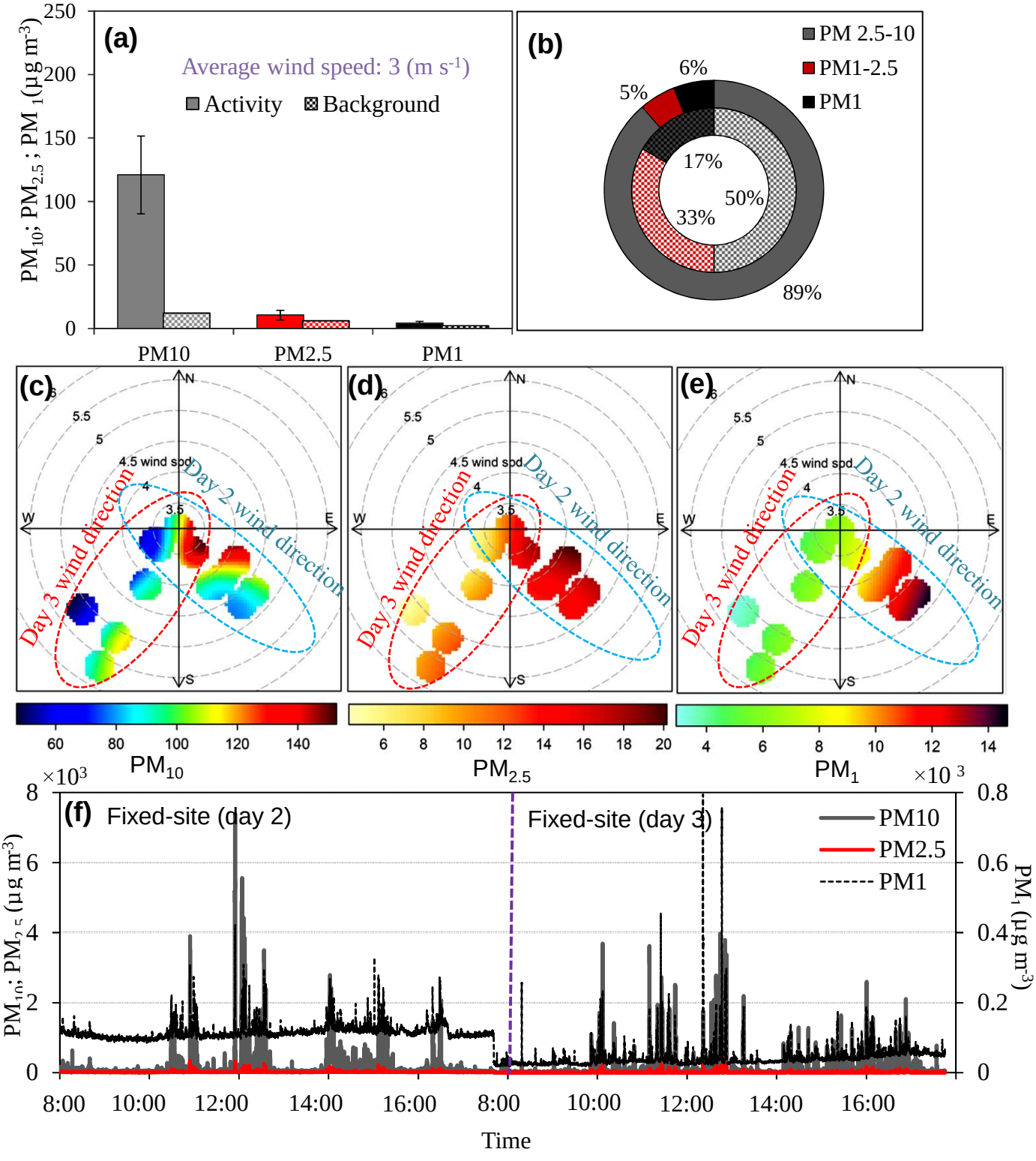
(a)
Average wind speed: 3 (m s-1)
Activity
Background
PM10; PM2.5 ; PM 1(µg m-3)
PM10
PM2.5
PM1
(b)
PM 2.5-10
PM1-2.5
PM1
6%
5%
17%
50%
33%
89%
(c)
(d)
(e)
4.5 wind spd
Day 2 wind direction
Day 3 wind direction
N
S
W
E
PM10
PM2.5
PM1
×10 3
(f)
Fixed-site (day 2)
Fixed-site (day 3)
PM10
PM2.5
PM1
PM10; PM2.5 (µg m-3)
PM1 (µg m-3)
Time

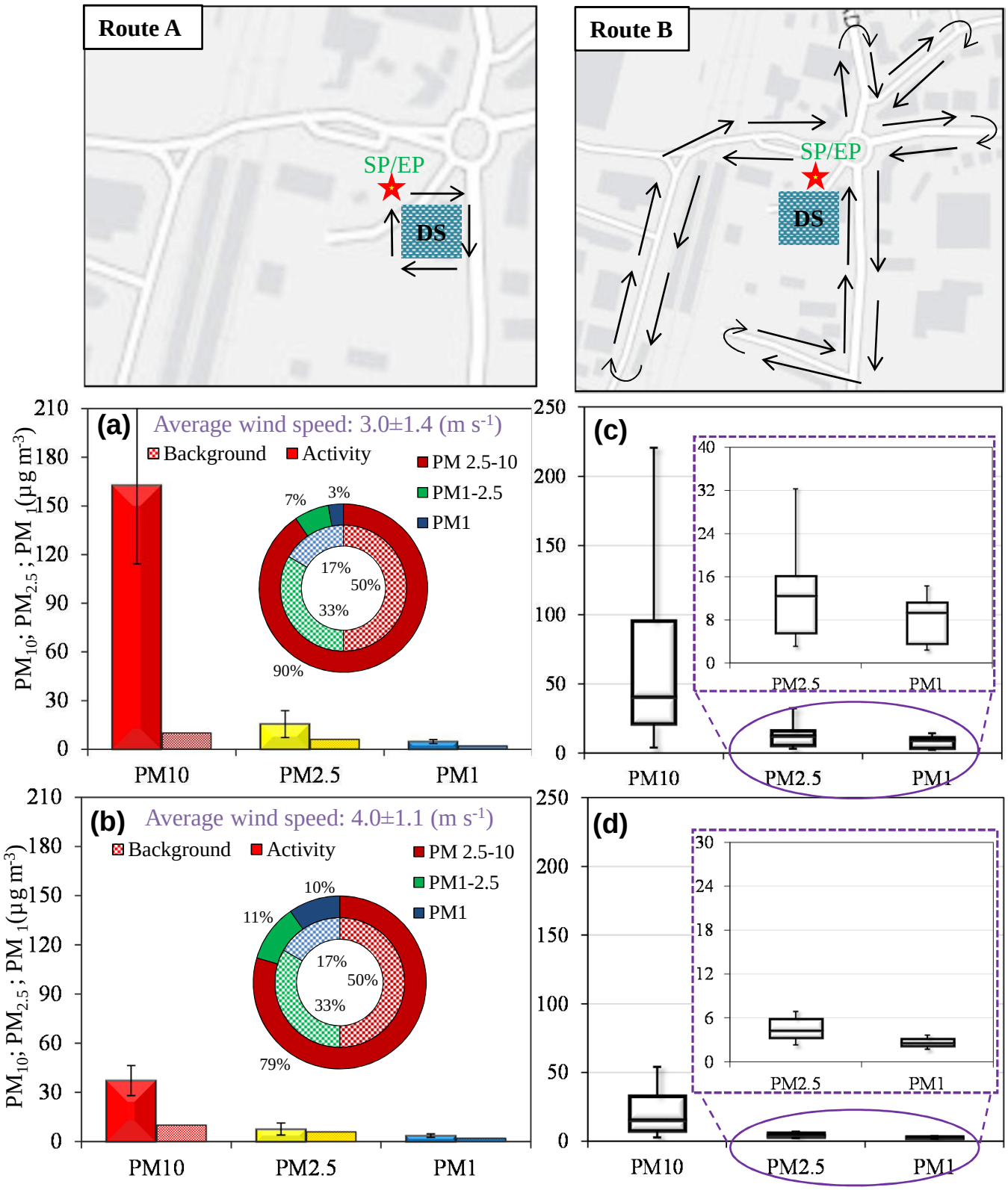
Route A
SP/EP
DS
Route B
SP/EP
DS
(a)
Average wind speed: 3.0±1.4 (m s-1)
Background
Activity
PM 2.5-10
PM1-2.5
PM1
7%
3%
17%
50%
33%
90%
PM10; PM2.5 ; PM 1(µg m-3)
PM10
PM2.5
PM1
(b)
Average wind speed: 4.0±1.1 (m s-1)
Background
Activity
PM 2.5-10
PM1-2.5
PM1
10%
11%
17%
50%
33%
79%
PM10; PM2.5 ; PM 1(µg m-3)
PM10
PM2.5
PM1
(c)
PM2.5
PM1
PM10
PM2.5
PM1
(d)
PM2.5
PM1
PM10
PM2.5
PM1

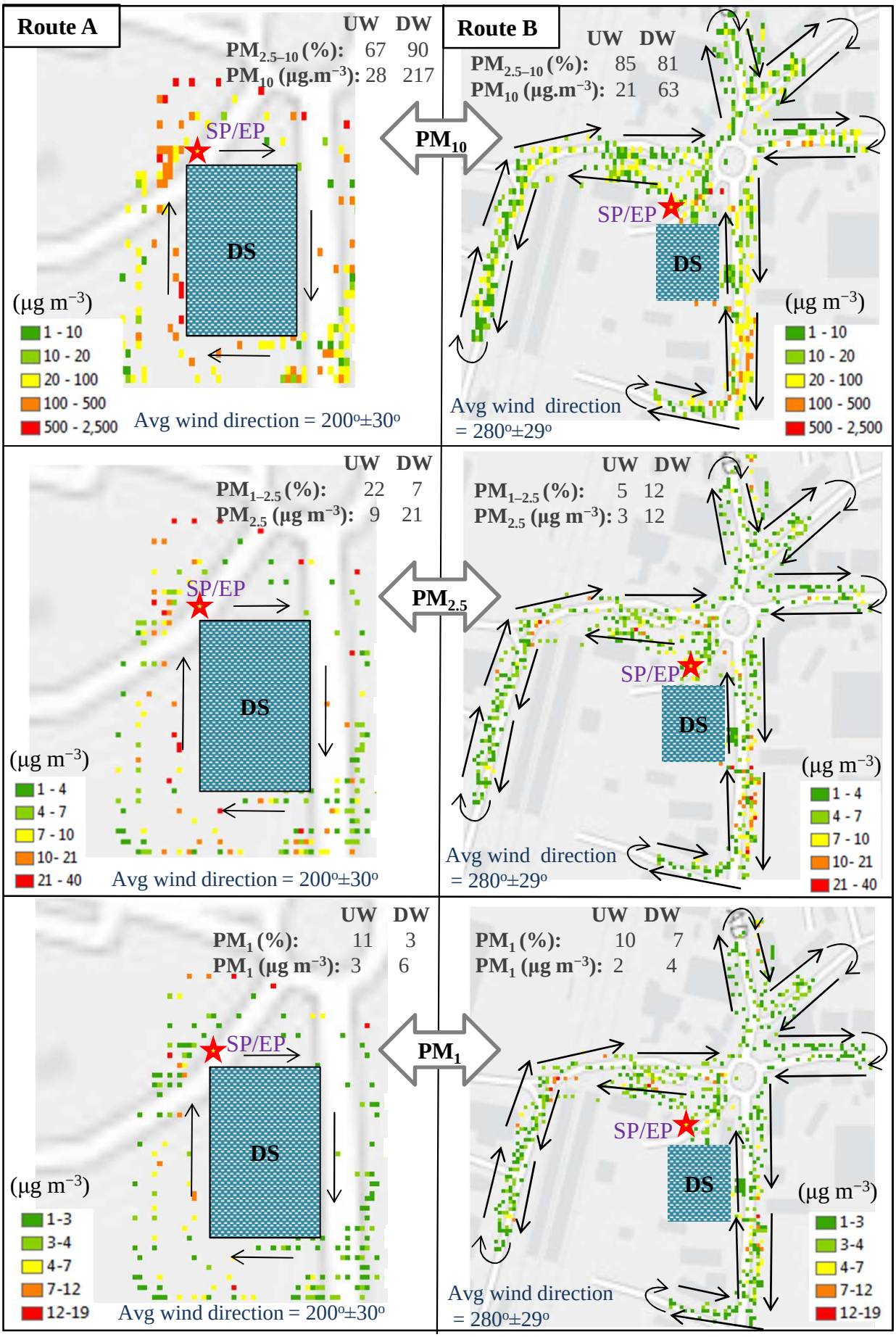
Route A
UW DW
PM2.5–10 (%): 67 90
PM10 (µg.m−3): 28 217
SP/EP
DS
(µg m−3)
1 - 10
10 - 20
20 - 100
100 - 500
500 - 2,500
Avg wind direction = 200º±30º
PM10
Route B
UW DW
PM2.5–10 (%): 85 81
PM10 (µg.m−3): 21 63
SP/EP
DS
(µg m−3)
1 - 10
10 - 20
20 - 100
100 - 500
500 - 2,500
Avg wind direction = 280º±29º
UW DW
PM1–2.5 (%): 22 7
PM2.5 (µg m−3): 9 21
SP/EP
DS
(µg m−3)
1 - 4
4 - 7
7 - 10
10- 21
21 - 40
Avg wind direction = 200º±30º
PM2.5
UW DW
PM1–2.5 (%): 5 12
PM2.5 (µg m−3): 3 12
SP/EP
DS
(µg m−3)
1 - 4
4 - 7
7 - 10
10- 21
21 - 40
Avg wind direction = 280º±29º
UW DW
PM1 (%): 11 3
PM1 (µg m−3): 3 6
SP/EP
DS
(µg m−3)
1-3
3-4
4-7
7-12
12-19
Avg wind direction = 200º±30º
PM1
UW DW
PM1 (%): 10 7
PM1 (µg m−3): 2 4
SP/EP
DS
(µg m−3)
1-3
3-4
4-7
7-12
12-19
Avg wind direction = 280º±29º

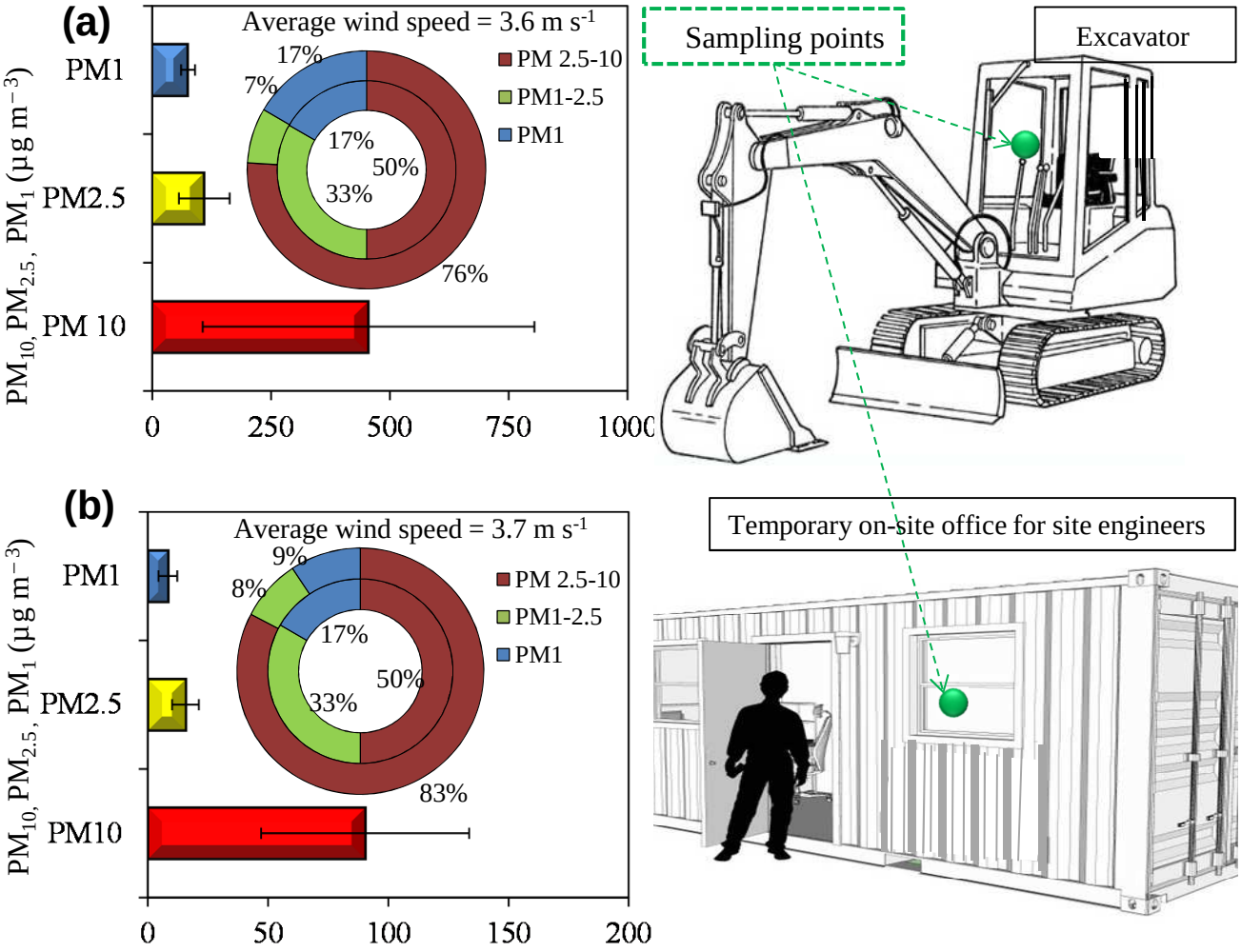
(a)
Average wind speed = 3.6 m s-1
PM1
PM2.5
PM 10
PM10, PM2.5, PM1 (µg m−3)
PM 2.5-10
PM1-2.5
PM1
17%
7%
17%
50%
33%
76%
0
250
500
750
1000
Sampling points
Excavator
(b)
Average wind speed = 3.7 m s-1
PM1
PM2.5
PM10
PM10, PM2.5, PM1 (µg m−3)
PM 2.5-10
PM1-2.5
PM1
9%
8%
17%
50%
33%
83%
0
50
100
150
200
Temporary on-site office for site engineers

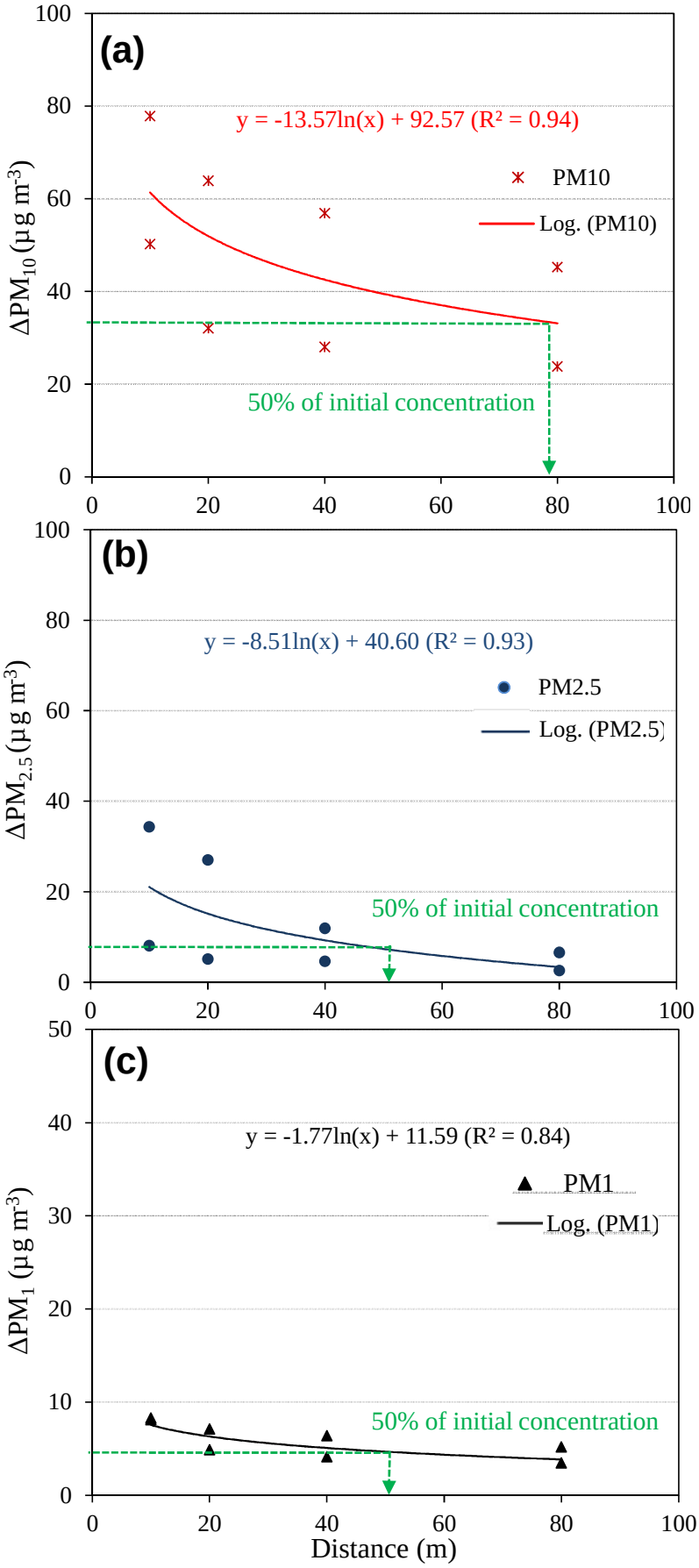
(a)
y = -13.57ln(x) + 92.57 (R² = 0.94)
PM10
Log. (PM10)
50% of initial concentration
ΔPM10 (µg m-3)
(b)
y = -8.51ln(x) + 40.60 (R² = 0.93)
PM2.5
Log. (PM2.5)
50% of initial concentration
ΔPM2.5 (µg m-3)
(c)
y = -1.77ln(x) + 11.59 (R² = 0.84)
PM1
Log. (PM1)
50% of initial concentration
ΔPM1 (µg m-3)
Distance (m)

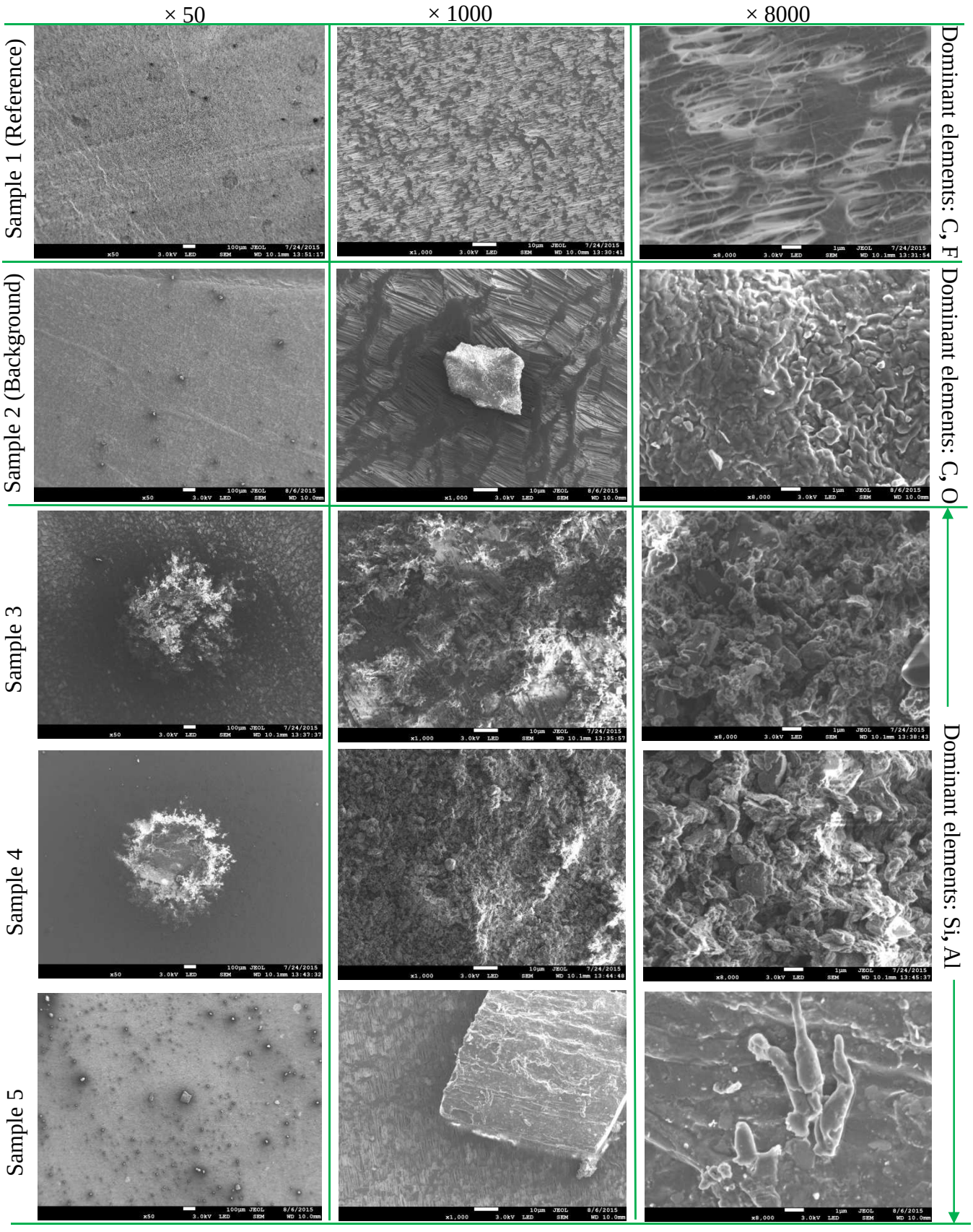
× 50
× 1000
× 8000
Sample 1 (Reference)
Sample 2 (Background)
Sample 3
Sample 4
Sample 5
Dominant elements: C, F
Dominant elements: C, O
Dominant elements: Si, Al

Research highlights

- PM_{10}, $PM_{2.5}$ and PM_1 concentrations from a building demolition are assessed
- Physicochemical properties of particles using SEM and EDS are investigated
- Average exposure doses increased by up to 57-times during the demolition activities
- PM profiles showed a logarithmic decay with increasing distance from demolition site
- Chemical analysis showed dominant concentrations of silicon and aluminium